

# Catalog of fundamental mode RR Lyrae stars in the Galactic bulge from the Optical Gravitational Lensing Experiment

Matthew J. Collinge<sup>1</sup>, Takahiro Sumi<sup>1</sup>, Daniel Fabrycky<sup>1</sup>

## ABSTRACT

We present a catalog of 1888 distinct fundamental-mode RR Lyrae stars detected in the Galactic bulge fields of the second phase of the Optical Gravitational Lensing Experiment (OGLE), covering an area near 11 deg<sup>2</sup>. These stars were selected primarily according to their light curve morphologies. The catalog includes basic parameters of the light curves, significant frequencies detected close to the main pulsation frequencies (characteristic of the Blazhko effect),  $V - I$  colors at minimum light (for most stars), and information useful for assessing the quality of the data for each star. We detect a high rate of incidence of the Blazhko phenomenon (at least 27.6%), including an unprecedentedly large proportion of stars with symmetrical frequency triplets, which we attribute to the new and sensitive method we employ to search for them. We find that the minimum light  $V - I$  color (useful as a reddening indicator) grows slowly redder with increasing period and exhibits an unexpectedly large star-to-star scatter of approximately 0.07 mag. We use this color to evaluate the zero-point accuracy of the reddening map of the Galactic bulge derived from OGLE data, and find that in addition to probable low-level random errors or resolution effects (responsible for much of the scatter), the map may systematically over-represent  $E(V - I)$  by approximately 0.05 mag in most fields. While the conclusion about the reddening zero points is somewhat tentative, we have reasonably robust evidence that the RR Lyrae-to-red clump color separation is larger by 0.05–0.08 mag in the bulge than locally; at a minimum this sounds a cautionary note about the use of these stars for reddening determinations until the effect is better constrained. We consider the RR Lyrae constraint on the Galactocentric distance, but our uncertainty about the absolute magnitude calibration and possible errors in the extinction determinations leave significant flexibility in the result. However, in contrast to previous results, we robustly detect the signature of the Galactic bar in the RR Lyrae population within the inner  $\pm 3^\circ$  of longitude, and we highlight the apparent differences between the structures traced by the red clump giants and the more metal-poor RR Lyrae stars.

---

<sup>1</sup>Princeton University Observatory, Princeton, New Jersey 08544, USA

## 1. Introduction

The photometric data sets obtained in the course of large microlensing surveys provide an abundance of opportunities to carry out scientific investigations not related to lensing. In one such project, Sumi (2004; S04 hereafter) presented extinction maps of the Galactic bulge fields observed in the Optical Gravitational Lensing Experiment (OGLE) during its second phase. These fields range in Galactic longitude between approximately  $-11 \text{ deg} < l < 11 \text{ deg}$  and cover an area close to  $11 \text{ deg}^2$ . The purpose of this effort was to enable studies of Galactic structure with the same data set.

The method employed by S04 was to determine the location of the red clump (RC) giants in the  $V - I, I$  color-magnitude diagram for a given sub-region of sky (presumably with homogeneous or nearly-homogeneous extinction), and use the observed color of the RC as a measure of the reddening. By locating the RC in the color-magnitude diagrams for sub-regions with different amounts of extinction, assuming the RC to be constant in luminosity as well as color, the reddening slope can be measured and extrapolated to zero reddening to obtain the total extinction (with some calibration). As suggested by Popowski (2000) and confirmed by Udalski (2003), S04 also found that the measured reddening slopes  $1.9 \lesssim R_{VI} \lesssim 2.1$  were significantly flatter than the “standard” value of about 2.5. Here  $R_{VI} \equiv A_V/E(V - I)$  is the usual ratio of total to selective absorption. This “anomalously” shallow extinction slope provides an explanation for previous claims (e.g., Stutz et al. 1999) that extinction corrected colors (derived according to a standard reddening law) of stars in the bulge were redder than their local counterparts.

The minimum light colors of fundamental mode RR Lyrae (RRab) stars have long been recognized as useful reddening measures (Sturch 1966) because of their low intrinsic dispersions and weak dependences on metallicity. The  $V - I$  color was suggested to be a particularly good reddening standard by Mateo et al. (1995) based on the data of Liu & Janes (1989). Recently, Day et al. (2002) and Guldenschuh et al. (2005) have studied the colors of field RR Lyrae stars and found the intrinsic minimum light color to be  $(V - I)_{0,ml} = 0.58 \pm 0.02$  (consistent with the value used by Mateo et al. 1995), with a scatter of 0.024 mag.

S04 considered the possibility that the intrinsic colors of RC stars might vary somewhat from field to field, due to a possible weak dependence on metallicity; in order to test this he compiled a list of RRab stars. In S04’s original analysis, the precision of the  $V - I$  colors of the RR Lyrae stars was limited, because the available  $V$ -band measurements were averages of small numbers of observations taken at random (and unknown) phases. In this work we present and analyze the catalog of RRab stars in the Galactic bulge. Using individual  $V$ -band time series, we extract measurements of  $(V - I)_{ml}$  for bulge RR Lyrae stars and use them to evaluate the field-to-field zero point accuracy of S04’s extinction map, among other

applications.

In §2 we discuss the OGLE data, in §3 we present the sample selection procedure, and in §4 we analyze the light curves. In §5 we extract and analyze the  $(V - I)_{ml}$  colors. In §6 we discuss the extinction zero points, distance scale, and geometry of the inner Galaxy, and in §7 we summarize our main conclusions.

## 2. OGLE observations and data sets

The data used in the present work were collected during the second phase of the OGLE project (OGLE-II hereafter). Details of the instrumental setup, calibration, and data pipeline can be found in Udalski et al. (2002; U02 hereafter) and references therein, who presented *BVI* photometric maps of the OGLE-II Galactic bulge fields. In addition to the photometric maps, we primarily make use of the *I*-band time series obtained through difference image analysis (DIA; Alard & Lupton 1998; Alard 2000) as presented by Szymański (2005), though our analysis is based on a somewhat older version of the reductions. DIA photometry for BUL\_SC28 were not available in these reductions, so our analysis is confined to the remaining 48 OGLE-II bulge fields. We also use the *V*-band time series, reduced via the standard (non-DIA) OGLE pipeline and kindly provided by the OGLE team. We transform the OGLE *V* and *I* magnitudes to the standard Johnson-Kron-Cousins system as prescribed by U02, after correcting for the low-level systematic flat-fielding errors mentioned in §5 of that work (M. Szymański 2004, private communication).

Two issues that can affect the utility of a photometric data set are the quality of the photometric error estimates and the choice of “good” frames. We adopt the following approach to these issues. On each frame, we construct a distribution of flux offsets for constant stars (chosen to have  $\chi^2$  per degree of freedom less than some threshold for a constant fit). We reject frames for which this distribution is significantly non-Gaussian, again based on a  $\chi^2$  threshold. For the remaining frames, we determine a scaling factor as a function of magnitude by which we multiply the photometric error estimates to allow accurate application of  $\chi^2$  fitting statistics. These procedures apply only to the *I*-band data; the much smaller number of *V*-band frames does not permit the same approach. Thus no error-scaling is performed for the *V*-band data points, and the choice of good frames is based on the standard OGLE data quality flags.

Since our analysis is based on non-public data, we performed several consistency checks to ensure that there were no major calibration problems as compared with published reductions of the same data sets. We compared the mean RR Lyrae magnitudes obtained from

the  $V$ -band time series with the same quantity as presented by U02. In the majority of cases, the mean  $V$  magnitudes we obtained agree with those presented by U02 to better than 1%; however, there are also tails to the  $\Delta V_{Up}$  (the subscript  $Up$  indicates a comparison between values from U02 and those from the present work) distribution that extend out to approximately  $\pm 0.2$  mag. These cases probably correspond to differences in the specific observations that were chosen to calculate the mean magnitudes; we applied a  $5\sigma$  filter before calculating the mean magnitudes for consistency with U02, but our implementation may differ slightly from that of U02, and we cannot guarantee that the choice of “good” frames is identical (a step that is performed prior to applying the  $5\sigma$  filter). Since the  $V$ -band light curves typically contain only 5–15 observations and typical amplitudes of RR Lyrae stars are several tenths of a magnitude or more, adding or subtracting a data point here and there can make a significant difference in the mean magnitude. Therefore we do not regard the width of the  $\Delta V_{Up}$  distribution as a matter for serious concern, especially since there is no evidence of a significant systematic offset between the two sets of magnitudes (mean  $\Delta V_{Up} \ll 0.01$ ). For the sake of caution, we exclude stars with  $|\Delta V_{Up}| > 0.1$  from subsequent analysis of the  $V - I$  colors.

We also compared the mean RR Lyrae magnitudes obtained from the DIA  $I$ -band time series against those presented by U02. Again we found no significant systematic offsets, and the root-mean-square (rms) difference in magnitudes for objects with  $|\Delta I_{Up}| < 0.2$  was  $\Delta I_{Up,rms} = 0.035$ . This is approximately the expected level of agreement. Although the  $\Delta I_{Up}$  distribution is somewhat narrower than the  $\Delta V_{Up}$  distribution (as expected since the number of observations in the  $I$ -band is much larger, and hence the impact of averaging over different subsets of the data is much smaller), there is still a slight tail of objects extending out to  $\pm 1$  mag. This can arise naturally because of crowding. If a star is blended with another star at close to the resolution limit of the survey, then it may be possible to separate the two on some frames but not others. Thus it may occur that the baseline magnitude obtained from DIA photometry may differ from the value obtained from standard point-spread-function (PSF) photometry, and the effect may have either sign. We suspect that this is the reason for objects with large values of  $|\Delta I_{Up}|$ . In any case such objects must be treated as suspicious; in the analysis of the  $V - I$  colors we exclude stars with  $|\Delta I_{Up}| > 0.1$ .

### 3. Selection of fundamental mode RR Lyrae

S04 selected 1961 RRab candidates from the OGLE-II catalog of variable stars in the Galactic bulge (Wozniak et al. 2002) using the method of Alard (1996). Periods were determined with the phase dispersion minimization technique (Stellingwerf 1978), and the  $I$ -band

light curves were decomposed as Fourier series of five harmonics. (For clarity, we remark that this modeling utilized the  $I$ -band data as presented by Wozniak et al. 2002, which differs from the reductions used elsewhere in the present work.) Among variables with periods shorter than 0.9 days, RRab candidates were selected as a clump in the  $\phi_{21}$ ,  $R_{21}$  plane. To avoid confusion arising from the window function imposed by the OGLE observing cadence, stars with periods in the range  $0.4985 < P < 0.5001$  day were excluded. According to convention,  $\phi_{21} \equiv \phi_2 - 2\phi_1$  and  $R_{21} \equiv A_2/A_1$ , where  $\phi_i$  and  $A_i$  are the phase (in radians) and amplitude of harmonic  $i$  in the Fourier series. Figure 10 of S04 shows the ellipse used to select the RRab candidates; the ellipse is centered on  $(4.5 \text{ rad}, 0.43)$  with semi-major axis  $a = 0.8$  and semi-minor axis  $b = 0.17$ , and the angle between the horizontal and the major axis is  $-10$  deg.

From the list of 1961 RRab candidates, we rejected redundant entries (5 stars), stars that had less than 25 data points in the  $I$ -band (26 stars, including all 13 RRab candidates in BUL\_SC28), one star that displayed an RR-Lyra-like light curve because it was blended with a true RR Lyra star, and 16 more stars that showed clear non-RR Lyrae light curves (e.g., constant light curves). Of the remaining 1913 RRab candidates, not all are unique; there are 25 stars that appear in the list twice because they lie in overlap regions between two fields. Because the number of multiply-identified stars is small and the duplicate data sets consist of independent measurements, we treat the duplicate entries independently in the analysis that follows. These stars provide a useful cross-check of the selection procedure and the overall photometric precision.

Figure 1 shows the distribution of periods. One can see a small dip near 0.5 day that results from the selection requirement mentioned above. The modal value of period indicated by the observed distribution is 0.56 day; after smoothing with a 5-bin boxcar filter, the peak shifts to 0.54 day, which appears somewhat more satisfactory to the eye. The mean period is intermediate between the two peaks at 0.552 day. This value indicates a similarity between RR Lyrae stars in the bulge and those found in Oosterhoff type I globular clusters (e.g., Smith 1995), as expected if the RR Lyrae stars in the bulge are on average relatively metal rich. Our mean period is consistent with the 0.554 day reported by Mizerski (2003), who also analyzed bulge RR Lyrae stars detected in OGLE-II. It is somewhat lower than the mean LMC RRab periods of 0.573 day obtained by Soszyński et al. (2003) and 0.583 day obtained by Alcock et al. (1996), and the mean SMC RRab period of 0.589 day obtained by Soszyński et al. (2002).

We present the list of 1913 RRab candidates (including the 25 duplicates) in Table 1, along with catalog identification numbers, mean photometry and equatorial coordinates from U02. The table also contains flags to warn of unreliable photometry, labels indicating any

multi-periodic nature as described in §4.1, and periods, amplitudes,  $I$  magnitudes at mean flux,  $V - I$  colors at minimum light, and  $\chi^2$  values derived from the modeling procedure discussed in §4.2. The 43 unique stars rejected from the sample are listed in Table 2 for completeness.

## 4. Analysis of the light curves

### 4.1. Frequency analysis

Many RR Lyrae stars display modulations of their light curves that are periodic or nearly so, with typical modulation periods in the range of tens to hundreds of days; these are the Blazhko stars (e.g., Smith 1995). In the frequency domain, the Blazhko effect can manifest itself as an additional significant peak or peaks close to the main pulsation frequency, with the difference in frequency corresponding to the modulation frequency. Two major subclasses are recognized in the literature: those having a single additional significant frequency, and those having two additional significant frequencies, one on either side of the main frequency. These two respective classes are sometimes termed BL1 and BL2, and it is often required that a frequency triplet be evenly spaced in order to receive the BL2 designation (e.g., Mizerski 2003). There are also Blazhko stars that do not conform to either class, having more than two or two unevenly spaced additional frequencies.

In order to identify Blazhko stars in our sample, we first pre-whiten the light curves by subtracting best-fit Fourier series of eight harmonics of the main pulsation period. (For details about Fourier analysis see §4.2.) Next we extract the frequency spectrum by running the CLEAN algorithm (Roberts et al. 1987) on the pre-whitened light curves for 200 iterations, with a gain of 0.5, on the frequency band  $[0-5 \text{ day}^{-1}]$  with a frequency resolution of  $0.125/T$ , where  $T$  is the overall time baseline of the observations. We sort the peaks and take the amplitude of the 15th largest peak ( $\mathcal{A}_{15}$ ) to be indicative of the noise level. The narrower the bandwidth searched, the less likely we are to find a spurious peak at a given amplitude. Since the different categories of secondary periodicities have different bandwidths, we determined a set of significance thresholds via a Monte-Carlo method described below. In what follows, we define the “Blazhko range” to be frequencies within  $0.1 \text{ day}^{-1}$  of, but separated by greater than  $1/T$  from, the main pulsation frequency. We exclude frequencies that are plausibly aliases (e.g., near-integer frequencies) from the classification scheme but include these frequencies in our noise estimates; this filter is required to guard against false positives induced by aliasing of low frequency noise, which our Monte-Carlo method overlooks. Only a small number of stars are classified more conservatively because of this filter.

To qualify as a BL1, a star must have a single peak in the CLEANed spectrum with amplitude  $\mathcal{A} > 2.4\mathcal{A}_{15}$  in the Blazhko range. In order to be considered a BL2, a star must have two frequencies within the Blazhko range (one on each side of the main pulsation frequency), with offsets from the main frequency that are identical to within  $3.0/T$ , and whose amplitudes both satisfy  $\mathcal{A} > 1.1\mathcal{A}_{15}$ . (The frequency condition follows the definition of an equidistant triplet found in Alcock et al. 2003). A star with more than one peak satisfying  $\mathcal{A} > 1.6\mathcal{A}_{15}$  within the Blazhko range but not satisfying the equidistant triplet condition is called “BL?”. BL2 and BL? classifications supersede BL1; a star satisfying the BL2 condition with an additional peak that satisfies the BL? condition is called “BL2+?”. Finally, a star with a peak satisfying  $\mathcal{A} > 1.39\mathcal{A}_{15}$  and within  $1/T$  of the main frequency is labeled PC for period change, following the discussion of Alcock et al. (2003). Such peaks may be indicative of a Blazhko period that is longer than the time baseline of the data set, but sometimes a star meets BL criteria as well, causing it to be labeled, for example, BL1+PC.

To refine the amplitude measurements for the additional significant frequencies, we used these frequencies to initialize a non-linear solver (the Levenberg-Marquardt algorithm; Press et al. 1989); the resulting frequencies and amplitudes are reported in Table 3. The best-fitting model was subtracted from the light curve and the amplitude of the highest remaining peak within  $0.1 \text{ day}^{-1}$  of the main frequency is also reported in Table 1. We do not consider this peak significant; it is reported to quantify the level of the noise for completeness studies. For BL1 stars we also report (in Table 3) the amplitude of the highest peak within the equidistant triple limits in frequency, which can be used to study the important question of whether the BL2 phenomenon makes a continuous transition to BL1.

The amplitude thresholds cited above were determined by a Monte-Carlo realization of the data set for each star, in which the magnitude residuals from the pre-whitening step were randomly swapped among the observation times. Next, the CLEAN algorithm was run and the amplitude thresholds of the routine to label the peaks were varied to produce an acceptable false alarm rate such that about 1% of the stars in each of the categories BL1, BL2, BL? and PC are likely to be spurious.

In addition to the expected BL1, BL2 and PC stars and stars displaying BL? behavior, our procedure allows us to identify several stars with double symmetrical frequency triplets (two sets of equidistant sidebands) in the Blazhko range. These stars have two pairs of peaks that both satisfy the BL2 conditions explained above. A similar phenomenon has been observed at least once before (LaCluyzé et al. 2004). We identify these 10 stars in Table 1 with the label BL2x2. While most of these stars exhibit a very closely spaced pair of frequencies on each side of the main pulsation frequency, which may indicate a BL2

phenomenon with unstable modulation frequency, there are also several interesting cases of stars showing two well-separated frequencies on each side of the main pulsation frequency. In contrast to expectation (e.g., Alcock et al. 2003), none of these frequency structures form evenly spaced quintuplets.

The number of unique stars in each of our categories is (BL1, BL2, BL?, BL2+?, BL2x2, PC) = (167, 282, 28, 37, 10, 119) = (8.8%, 14.9%, 1.5%, 2.0%, 0.5%, 6.3%). While we have confidence in the robustness of our detections of additional significant frequencies, many are close to the limits of our ability to detect them, which indicates that we may still be missing a significant proportion of Blazhko stars. Among the 25 stars detected twice in overlapping fields, 10 of which are classified as having some type of BL/PC behavior, eight of the duplicate data sets receive different classifications. Two of these are cases of stars switching from one BL category to another because of the detection of an additional peak in one of the data sets (these stars contribute twice to the numbers listed above); the remaining six stars are simply not recognized as BL/PC in one of the data sets. In all cases, the amplitudes of the extra peaks are close to the noise levels of the data sets in which the extra peaks were not detected. Thus there is no conflict with our estimate of completeness for each data set, but this underscores the fact that more Blazhko stars remain to be discovered in our sample.

Despite the likely incompleteness of our Blazhko classifications, we have detected a very high rate of incidence of the Blazhko phenomenon compared to previous studies. Overall  $522/1888 = 27.6\%$  of our unique stars display some sort of Blazhko behavior (not including stars with only PC labels) and an additional 4.8% are classified solely as PC stars. The former number is somewhat larger than the total Blazhko incidence rates of  $\sim 23\%$  reported by Moskalik & Poretti (2003) and 24.3% reported by Mizerski (2003) for RRab in the bulge; the 24.3% breaks down into 12.5% BL1, 7.4% BL2 and 4.4% BL?, with an additional 0.7% possible PC stars. The incidence rate in the LMC was reported to be 11.9% by Alcock et al. (2003), which breaks down into 6.5% BL1, 5.4% BL2 and 0.3% BL?, as well as a separate 2.9% PC incidence rate. The fact that our overall Blazhko incidence rate exceeds that of Mizerski (2003) (unlikely to be simple counting statistics, considering the sample sizes) may be attributed to the greater number of observations in our data set as compared to his (four seasons instead of three) and our different search procedure, resulting in the somewhat greater sensitivity of our search. It has been suggested that the Blazhko effect is more prevalent in the bulge than in the LMC because of the different metallicities (e.g., Moskalik & Poretti 2003). But leaving that question aside, what is most striking is the much higher proportion of BL2/BL1 stars among our classifications as compared to the previous studies. Since we believe our detections to be robust, we suggest that this simply owes to our method, which greatly increased our sensitivity in the narrow bands associated with BL2 and PC behavior, allowing us to push far down into the noise to recover them.



## 4.2. I-band models

In order to reliably extract information such as the magnitude at mean flux, the overall amplitude, and the behavior of the light curve during the minimum light interval, some degree of modeling is required. However, seeking to provide a faithful representation of the complex multi-periodic light curves exhibited by the Blazhko stars is beyond the scope of the present work. After consideration of many alternatives, we decided to adopt the simplistic approach of modeling the *I*-band light curves as singly-periodic Fourier sums of only six harmonics. That is, we adopted a model of the form

$$f(t) = f_0 + \sum_{k=1}^6 [A_k \cos(2\pi kt/P) + B_k \sin(2\pi kt/P)] \quad (1)$$

where  $P$  is the period and  $f$  indicates that all fitting was performed in terms of fluxes. Thus the magnitude  $I_{\text{mf}}$  at mean flux corresponding to  $f_0$  can be extracted directly from the light curve. The values of  $I_{\text{mf}}$  in Table 1 have been transformed to the standard photometric system assuming that the intrinsic mean  $V - I$  color of RR Lyrae stars is 0.45 (reddened according to S04); this was necessary because we do not have good measurements of the average  $V$ -band magnitude of many stars. The amplitudes given in Table 1 represent the minimum-to-maximum range (in mag) of the model.

We chose six harmonics because this is enough to capture the essential shape of the light curve, but few enough to avoid over-fitting even of particularly badly behaved stars. Since some light curves contain individual (or small numbers of) highly discrepant points that can affect the fits, we implemented a procedure to trim outlying points that deviated by more than  $5\alpha_\chi\sigma_i$ . Here  $\alpha_\chi$  is the rms value of  $(f_i - m_i)/\sigma_i$ , where  $f_i$ ,  $m_i$  and  $\sigma_i$  are the observed flux, model flux and photometric error for data point  $i$ . All fits were inspected to ensure that they had converged to visually reasonable approximations of the light curves.

As can be readily seen from the fact that most of the  $\chi^2/\nu$  (where  $\nu$  is the number of degrees of freedom) values presented in Table 1 are much larger than unity, the six-harmonic Fourier models do not provide formally acceptable fits to the light curves. In some cases it is possible to achieve  $\chi^2/\nu \approx 1$  fits by increasing the number of harmonics; however, such a procedure needs to be tightly supervised to avoid unreasonable behavior. Moreover, a significant fraction of the stars simply cannot be represented by a model with a single, constant frequency (and its harmonics), so we do not include the results of higher-harmonic fits in this paper. Many of the stars that are intractable to single frequency models are Blazhko stars or PC stars, but some are not; detailed investigation of these cases is beyond the scope of the present paper. Example light curves and *I*-band models are shown in Figure 2.

Figure 3 shows the relationship between  $I$ -band amplitude and period, also known as the Bailey diagram, displaying the expected anti-correlation between the two quantities. Visual comparison of Figure 3 with Figure 8 of Soszyński et al. (2003), who presented the OGLE catalog of RR Lyrae stars in the Large Magellanic Cloud, reveals no striking differences between their RRab sample and ours, other than the relative numbers. Such comparison also demonstrates that the contamination of our sample by non-fundamental mode RR Lyrae stars is negligible. Nine stars from our sample are not shown in Figure 3 because they have anomalously large amplitudes in the range 1.1–2.8. These stars are unexpectedly faint, with an average  $I$  magnitude of 17.5 as compared with the sample average of 16.2, and six of nine have  $\Delta I_{Up} > 0.1$ . We suspect these are cases in which the baseline DIA magnitude has been set erroneously faint, possibly because of blending (i.e., flux from the variable star has been mistakenly assigned to a nearby blended star), resulting in implausibly large variability amplitudes. In any case we exclude these stars from the analysis in §5. We also comment that among the seven stars with variability amplitudes below 0.1 mag, the average  $I$  magnitude of 14.3 is rather bright; some or all of these are likely to be unresolved blends, leading to the bright apparent magnitudes and low variability amplitudes. We address this and other confusion effects in the next section.

## 5. $(V - I)$ at minimum light

The minimum light interval is usually defined to be phases of 0.5–0.8 after maximum light (e.g., Guldenschuh et al. 2005). Here the phase has been normalized by  $1/2\pi$  and ranges from 0–1. Since we have typically only 5–15  $V$ -band measurements per star taken at random phases, some stars in our catalog do not have  $V$ -band measurements in this interval. A further complication is that OGLE observations in  $V$  and  $I$  are by no means simultaneous. Since there is in general no data point in  $I$  sufficiently close in time to a given data point in  $V$ , we use the light curve models discussed in the previous section to extract estimates of the  $I$ -band magnitude at the time corresponding to a given  $V$ -band observation. We estimate the error on the  $V - I$  measurements so obtained to be

$$\sigma_{V-I}^2 = \sigma_V^2 + \frac{\sum_{i=1}^m (I_{obs} - I_{model})^2}{m(1 - \nu/N)}, \quad (2)$$

where the sum over  $i$  includes the  $m$  observations in  $I$  within a phase interval of  $\pm 0.05$  around the  $V$ -band measurement,  $\nu$  is the number of degrees of freedom in the fit, and  $N$  is the total number of  $I$ -band measurements. For stars that have several  $V$  data point in the minimum light interval, we combine them to obtain a single best estimate of  $(V - I)_{ml} = [\sum (V - I) / \sigma_{V-I}^2] / \sum 1 / \sigma_{V-I}^2$  with its accordant error.

From the ensemble of  $V - I$  data points that fall in the minimum light interval, it is possible to discern a slight dependence on phase, in the sense that the color becomes slightly bluer with increasing phase; however this effect is weak (total change in  $V - I$  at the level of 0.01 through the 0.5–0.8 phase interval) and we neglect it in what follows.

### 5.1. Extracting a clean subsample

Taken at face value, the  $V - I$  data points obtained as described above include a significant proportion of measurements that are inaccurate for one reason or another, such as blending. We outline below the series of cuts we apply to go from our full sample of 1913 stars to the final data set of 1106 stars that yield useful measurements of the  $V - I$  color at minimum light. These cuts are presented in succession, so the number of stars rejected by the cuts as given below corresponds to the number of additional stars rejected after the preceding cuts have already been applied.

1. 214 stars have no  $V$  observation in the minimum light interval, defined to be phases between 0.5–0.8 with respect to maximum light.
2. Seven stars have extinctions from S04 above the reliability threshold of  $A_I > 2.9$ .
3. 258 stars are predicted to have  $V$  magnitudes at minimum light that are below the detection limit of  $V_{lim} \approx 20.5$ . The  $V_{ml}$  magnitudes are predicted from the  $I$ -band light curve by adding the assumed intrinsic, minimum light color  $(V - I)_{0,ml} = 0.58$ , reddened according to S04.
4. 62 stars have  $I_{mf} < 13.7 + (V - I)_{ml}$ , that is, they are more than 0.7 mag brighter than the approximate reddening line (of slope unity, within the range of observed values from S04)  $I_{mf} = 14.4 + (V - I)_{ml}$  that characterizes the bulk of the sample. The observed color-magnitude diagram for RR Lyrae stars is shown in Figure 4. The 62 stars excluded by this cut may include foreground stars, which may or may not be subject to the same amount of extinction as stars in the bulge, and stars with significant blending.
5. 53 stars have  $I_{mf} > 15.1 + (V - I)_{ml}$ , that is, they are more than 0.7 mag fainter than the “sample” reddening line defined above. These may include background stars, which could be subject to more extinction than stars in the bulge, and stars with zero-point errors as discussed in §4.2.

6. 44 stars have  $|\Delta I_{Up}| \geq 0.1$ , indicating that they may have unreliable  $I$ -band photometry.
7. 56 stars have  $|\Delta V_{Up}| \geq 0.1$ , indicating that they may have unreliable  $V$ -band photometry.
8. 107 stars have  $\sigma_{V-I,ml} \geq 0.1$ , indicating that they are close to the detection limit in  $V$  or that the quality of the fit to the  $I$ -band light curve is especially poor.
9. Six stars have  $(V-I)_{0,ml}$  more than  $5\sigma$  away from the sample average (after application of all preceding cuts), where  $\sigma = 0.079$  mag is the rms deviation around the mean.

The resulting sample of 1106 stars has  $\langle (V-I)_{0,ml} \rangle = 0.528 \pm 0.002$ . One can immediately notice that this value and the standard deviation quoted above differ significantly from the results of Guldenschuh et al. (2005), who found  $(V-I)_{0,ml,av} = 0.58 \pm 0.02$  with an rms scatter of  $\sigma = 0.024$ ; this discrepancy is discussed in §6.

## 5.2. Dependence on other properties

We searched for correlations between  $(V-I)_{0,ml}$  (dereddened according to S04) with other basic parameters: period, amplitude, and the Fourier phase differences  $\phi_{21} \equiv \phi_2 - 2\phi_1$  and  $\phi_{31} \equiv \phi_3 - 3\phi_1$ . The latter two quantities were included because it has been suggested that in combination with period, these phases can be used to determine metallicity. Following the original proposal by Kovács & Zsoldos (1995), Jurcsik & Kovács (1996) presented a linear relationship between metallicity, period, and  $\phi_{31}$  determined from the  $V$ -band light curve; recently Smolec (2005) presented a similar relationship calibrated in the  $I$ -band.

We found statistical and visually significant relationships between  $(V-I)_{0,ml}$  and all of the other basic parameters. However, the interpretation of these relationships is ambiguous since to varying degrees period, amplitude,  $\phi_{21}$  and  $\phi_{31}$  all correlate (or anti-correlate) with one another. In order to disentangle these dependences, we performed the following simple test. We searched for linear relationships between  $(V-I)_{0,ml}$  and period (or  $\log P$ ) and corrected the  $(V-I)_{0,ml}$  values to a fiducial period. We then searched for correlations between these corrected  $(V-I)_{0,ml,cor}$  values and amplitude,  $\phi_{21}$  and  $\phi_{31}$ .

As it turns out, unweighted linear least-squares regression produces a relationship between  $(V-I)_{0,ml}$  and  $\log P$ ,

$$(V-I)_{0,ml} = (0.525 \pm 0.004) + (0.30 \pm 0.06)(\log P + 0.263), \quad (3)$$

that is sufficient to account for virtually all of the correlations between  $(V - I)_{0,ml}$  and the other quantities. This relationship is shown in Figure 5. After correcting  $(V - I)_{0,ml}$  to the fiducial period of 0.546 day ( $\log P = -0.263$ ), we compute Spearman’s rank-order correlation coefficients  $r_s$  for the remaining relationships between  $(V - I)_{0,ml,cor}$  and amplitude,  $\phi_{21}$  and  $\phi_{31}$ . The results are  $r_s = -0.063$ , 0.041 and 0.048 respectively, with corresponding null hypothesis probabilities (NHPs) of 3.6%, 17.6% and 11.3%. For comparison, the original correlations between  $(V - I)_{0,ml}$  and the other quantities all have NHPs  $\ll 0.001\%$ , meaning that they are all significant at much greater than 99.999% probability. While it may be that weak relationships remain after taking out the dependence on period, at such low significances, it practically goes without saying that any remaining correlations between the quantities are invisible to the eye.

If one accepts that RR Lyrae metallicities can be determined from the light curves, the fact that the relationships between  $(V - I)_{0,ml}$  and other observables can be reduced to a simple relationship with period suggests that any direct dependence of  $(V - I)_{0,ml}$  on metallicity should be very weak. This is consistent with the result of Guldenschuh et al. (2005) who found at most a weak dependence of  $(V - I)_{0,ml}$  on metallicity.

We also checked for any systematic difference of  $(V - I)_{0,ml}$  between singly-periodic RRab and Blazhko stars. The 294 Blazhko stars that yield usable measurements of  $(V - I)_{0,ml}$  prefer a slightly bluer color than the full sample: 0.519 as compared with 0.528, whereas there is no significant difference in the mean periods. However, the scatter in  $(V - I)_{0,ml}$  among both Blazhko and non-Blazhko stars is much greater than the difference in the mean values, and in any case the difference is small, and the inclusion of the Blazhko stars does not greatly affect the overall sample mean.

### 5.3. Field-to-field variations

Based on the analysis of  $V - I$  colors obtained from the photometry of U02 for RR Lyrae stars, S04 found tentative evidence that the zero-point of his reddening maps systematically differed for fields with Galactic longitudes  $l$  significantly away from zero; the sense of the effect was that extinction corrected RR Lyrae colors appeared redder by  $\sim 0.1$  mag for fields with large  $|l|$  (see his Figure 12). In Figure 6 we can also see a hint of redder colors at the extremes in Galactic longitude; though the scatter of our points is somewhat smaller than S04’s, the trend is no more clear in that the average colors in fields with large  $|l|$  themselves display a large scatter. This is partly because the numbers of RR Lyrae stars are relatively low in these fields. Indeed, as the upper panel of Figure 7 shows, the redder  $\langle (V - I)_{0,ml,cor} \rangle$  colors are concentrated in fields with relatively low stellar densities, as traced by the RR

Lyrae population. The data from Figures 6 and 7 are given in Table 4.

## 6. Discussion

### 6.1. Relative zero points and discrepancy with field RRab colors

In addition to the apparent dependence of the reddening zero point on environment, the discrepancy of 0.05 mag between the mean value of  $(V - I)_{0,ml}$  for RRab stars in our sample and the field RRab value obtained by Guldenschuh et al. (2005) has interesting implications. Since the reddening map of S04 was obtained by assuming that the intrinsic color of the RC in the bulge is the same as its local color, the 0.05 mag color offset actually represents a discrepancy between the RR Lyrae-to-RC color differential in the bulge as compared to its local value. Caution must be employed in trying to interpret this discrepancy, however, because systematic errors in the OGLE photometry may appear at approximately this level (A. Udalski 2005, private communication). While the possibility of systematic errors in the photometry complicates the interpretation of this discrepancy, what would be needed to remove it entirely would be color-dependent systematic errors, which are somewhat more difficult to arrange.

One possible source of color-dependent systematic errors is the non-standard red wing of the OGLE  $I$ -band filter. The linear transformation presented by U02 to convert between OGLE magnitudes and Johnson-Kron-Cousins magnitudes becomes increasingly inadequate for redder stars. U02 calculated that this error should not exceed about 0.03 mag for stars with  $V - I < 2$ , but it is non-linear in its dependence on color and may reach almost 0.2 mag for  $V - I \approx 4$ . The sign of the effect is that, for red stars, the  $V - I$  colors derived from OGLE observations (after the photometric transformation has been applied) will be redder than the true colors, and the  $I$ -band magnitudes will be correspondingly too bright. Thus for heavily reddened fields, the reddening as measured by S04 may be systematically too large and the dereddened RR Lyrae colors artificially blue. However there are several problems with this explanation. The first is that the color offset between RC and RR Lyrae stars introduced by this phenomenon is a first-order correction to an already small effect, accounting for at most about 0.02 mag of the discrepancy for  $E(V - I) < 1$  (judging from Figure 2 of U02). On top of this, the calculations of U02 neglect atmospheric absorption, which as they note would mitigate the errors to some degree. Another problem is that, since the systematic errors resulting from the red wing increase non-linearly for progressively redder stars, we would expect the color discrepancy to grow with increasing reddening, whereas there is no signature of this in the lower panel of Figure 7. Thus we conclude that systematic errors caused by the red wing are unlikely to be responsible for the observed color discrepancy.

A second possible source of systematic errors is unresolved stellar blends in the denser fields. The fact that the  $(V - I)_{0,ml}$  colors of RRab stars in the less dense fields are closer to the local colors argues that possible problems related to crowding should be considered. However, the pixel-level simulations of Sumi et al. (2006) cast doubt on whether blending is a significant effect for stars as bright as RR Lyrae and RC giants (see their Figure 6), though it may be responsible for a relatively small number of magnitude outliers. A bigger problem with the blending hypothesis is that RR Lyrae and RC stars have comparable brightnesses, and therefore the populations of stars available to blend with them are practically indistinguishable. This means that on average blending should bring their colors closer together rather than pushing them farther apart. This is the wrong sign to explain the observed color discrepancy, so blending cannot be the source of the effect.

One additional factor that influences the color discrepancy is the overall zero point calibration of S04’s extinction map. S04 used independent measurements of  $A_V$  for 20 RRab stars in Baade’s Window to determine that on average his RC-color method slightly overestimated the extinction, and consequently he applied small corrections to his reddening and extinction values. This correction amounts to a reduction in  $E(V - I)$  of only 0.028, but if it had not been applied we would have observed a larger color discrepancy, and hence it is relevant.

Since we have eliminated what seem like the most plausible artificial causes for the RR Lyrae/RC color discrepancy, the most probable conclusion is that it is real. Such a population difference, amounting to 0.05-0.08 mag in  $V - I$  between the bulge and the local region of the Galaxy, would not be very surprising. Unfortunately it is difficult to determine whether the effect is confined to the RC or to the RR Lyrae, or whether both classes of star are subject to population effects. At present there exists only marginal evidence for a dependence of  $(V - I)_{ml}$  on metallicity for the RR Lyrae (Guldenschuh et al. 2005). While the tentative trend has the correct sign to explain part of the color discrepancy (assuming the bulge RR Lyrae to be more metal-rich than the local ones), its slope is much too shallow to account for all of it. Any difference between the average period of the field RRab stars and the average period of our sample is far too small to account for the effect through equation 3. It may be that population effects are more important for the RC than for the RR Lyrae, but further studies of local RR Lyrae colors are needed before this can become a strong statement. In any case the color inconsistency indicates that the zero-point calibration of S04’s reddening map should be treated as uncertain at the level of 0.05 in  $E(V - I)$ .

Another discrepancy between the minimum light colors of bulge and field RRab stars is in the star-to-star scatter. Guldenschuh et al. (2005) quote an rms scatter of only 0.024 mag, whereas the standard deviation measured from our sample is 0.079 mag. For comparison,

a typical value of the photometric uncertainty  $\sigma_{V-I}$  in the minimum light interval for our sample is 0.045 mag. Accounting for the observed dependence on period does not significantly reduce the scatter of our observed colors, nor is the scatter within most individual fields (0.07 mag on average for fields with more than five RRab stars) significantly less than in the overall sample. This star-to-star variation may reflect low-level random errors in the reddening map or errors resulting from unresolved structure in the extinction, or it may be that the intrinsic scatter in  $(V - I)_{ml}$  has been underestimated because of the small number of field RRab studied.

## 6.2. RC and RR Lyrae magnitudes in Baade’s window

Another problem noted by S04 is that the extinction corrected  $I$ -band magnitude of the RC in Baade’s window (BW) is 14.6; the BW data were chosen merely to illustrate the point and do not conflict with adjacent fields. The expected apparent magnitude is 14.3, assuming that the absolute magnitude is  $M_{I_{0,RC}} = -0.26 \pm 0.03$  (Alves et al. 2002) (from *Hipparcos*) and if the Galactic center (GC) distance modulus is  $14.5 \pm 0.1$  (corresponding to 7.94 kpc, as given by Eisenhauer et al. 2003; the BW distance modulus differs from that of the GC by only about  $-0.02$  mag according to Paczyński & Stanek 1998). Since the  $V$ -band magnitude of RR Lyrae stars is a reasonably good standard candle, we can check for a similar effect. For the 158 RR Lyrae in BW that satisfy  $A_I \leq 2.9$ ,  $V_{Udal} < 20.5$ ,  $|\Delta V_{Up}| < 0.1$ , and  $13.6 + 2(V - I)_{ml} \leq V_{Udal} \leq 15.1 + 2(V - I)_{ml}$  (similar to the requirements from §5.1, but adapted to the  $V$ -band; for stars that lack  $V$  observations in the minimum light interval, we assume  $(V - I)_{0,ml} = 0.58$ , reddened according to S04’s map) we obtain  $\langle V_{0,Udal} \rangle = 15.46 \pm 0.04$ , where the subscripts “Udal” and “0” respectively indicate that we are using mean magnitudes as presented by U02, corrected for extinction according to S04. The field-to-field scatter of  $\langle V_{0,Udal} \rangle$  within BW is more like  $\pm 0.1$  mag, so we adopt this as the approximate level of accuracy. We subtract a small correction of 0.03 mag to account for the fact that these are mean magnitudes rather than magnitudes at mean flux; this correction was determined based on the  $I$ -band light curves and assuming a typical  $V$ -band amplitude of about one mag. We note that since the zero point of S04’s extinction map is fixed according to absolute extinction rather than color, a reddening zero point correction as suggested in §6.1 would not automatically affect the derived values of extinction. Thus we obtain  $\langle V_{0,mf} \rangle = 15.43 \pm 0.1$  for the BW RR Lyrae stars.

Though the  $I$ -band luminosities of RR Lyrae stars are not as well calibrated, the OGLE  $I$ -band data have many advantages compared to the  $V$ -band. For the 158 stars that pass requirements 2, 4, 5 and 6 from §5.1 (differing by only 5 stars from the 158 stars used to



compute  $\langle V_{0,Udal} \rangle$ ), an unweighted linear least-squares regression yields

$$I_{0,mf} = (-1.6 \pm 0.3)(\log P + 0.263) + (14.99 \pm 0.02). \quad (4)$$

The mean extinction corrected  $I$ -band magnitude is  $\langle I_{0,mf} \rangle = 14.97 \pm 0.02$  (statistical). The slope of the relation is consistent with the value of  $-1.62$  reported by Soszyński et al. (2003) for the LMC RR Lyrae. However the current lack of a good calibration of  $M_I$ , especially its metallicity dependence, precludes our relying on the  $I$ -band data in what follows.

If we adopt the RR Lyrae absolute magnitude of  $M_V = 0.59 \pm 0.03$  at  $[Fe/H] = -1.5$  as compiled by Cacciari & Clementini (2003) and assume a metallicity dependence of  $M_V = (0.25 \pm 0.05)[Fe/H] + constant$  (consistent with the range of slopes found in the literature), then using the average metallicity of  $[Fe/H] = -1$  from Walker & Terndrup (1991), we obtain  $M_V = 0.72 \pm 0.04$  for RR Lyrae stars in BW. This predicts  $\langle V_{0,mf} \rangle = 15.2 \pm 0.1$  for BW RR Lyrae; in other words with this RR Lyrae calibration we obtain a similar discrepancy for RR Lyrae stars to that which S04 obtained for RC stars, though of somewhat lower statistical significance. But bearing in mind that this offset is seen in the  $V$ -band whereas S04’s RC discrepancy is in the  $I$ -band, any implication for the overall extinction zero point is far from clear. Alternatively if we adopt the RR Lyrae statistical parallax calibration of  $M_V = 0.77 \pm 0.13$  at  $[Fe/H] = -1.6$  from Gould & Popowski (1998), then using the same metallicity dependence we predict  $M_V = 15.42 \pm 0.16$  for RR Lyrae stars in BW. This is uncomfortably close to the observed value. If the fainter RR Lyrae calibration is nearer to the truth, it would seem to indicate that the source of the RC magnitude discrepancy is intrinsic to the RC (such as a population effect); however the lingering uncertainties in the RR Lyrae absolute magnitude calibration prevent us from reaching a firm conclusion.

### 6.3. The Galactic bar as traced by RC and RR Lyrae stars

While the absolute magnitude calibrations of RC and RR Lyrae stars may be debated, their utility as relative distance indicators (modulo population effects) is robust. In Figure 8, we show the mean extinction corrected magnitudes of RC and RR Lyrae stars as functions of Galactic coordinates, grouped into regions A–K following S04. In calculating the mean RR Lyrae magnitudes, we have applied the same requirements described in §6.2 for the  $V$ -band, and equivalent criteria for the  $I$ -band. The signature of the Galactic bar is clearly visible in the inner fields ( $|l| < 3^\circ$ ) as a trend from brighter to fainter apparent magnitude going from positive to negative Galactic longitude. The strength of this trend as reflected in the RR Lyrae population stands in contrast to the result of Alcock et al. (1998), who found only weak evidence for a bar in the RR Lyrae population; however, our data do support

the conclusion of Alcock et al. (1998) that the bar signature in the RR Lyrae population is present only in the inner fields. The fact that the slope of magnitude versus longitude appears somewhat shallower for the RR Lyrae as compared to the RC stars may reflect a contribution to the RR Lyrae population from the inner Galactic halo.

In addition to the signature of the bar in the inner fields, several other features of Figure 8 deserve mention. As noticed by S04, the fields above the Galactic plane seem to differ from the longitudinal trends displayed by the remaining fields, though the significance of this effect is lower for the RR Lyrae stars. Also interesting is the fact that while both the RC and RR Lyrae magnitudes appear to recover toward the mean values for  $l < -5^\circ$  (though perhaps by different amounts), the two populations appear to diverge for  $l > 4^\circ$ , with the RR Lyrae magnitudes recovering toward the mean and the RC magnitudes continuing to brighten. The reasons for these asymmetries are not currently clear, but they may have important implications for the structure of the central Galaxy.

## 7. Conclusions

We have presented a catalog of 1888 fundamental mode RR Lyrae (RRab) stars extracted from the OGLE-II Galactic bulge data set, plus 25 double entries of stars detected in two fields for a total of 1913 entries. The catalog includes basic light curve parameters such as periods, amplitudes, mean magnitudes,  $V - I$  measurements at minimum light, labels to indicate Blazhko phenomenology, and significant additional frequencies detected close to the main pulsation frequency, as well as extinctions derived from the map of S04 and various additional information useful for assessing the quality of the photometric data for individual stars. This data set has a variety of applications for studies of the inner Galaxy.

Our frequency analysis (§4.1) of the light curves has revealed a high incidence of the Blazhko phenomenon: 27.6% of the stars show some type of clear Blazhko behavior and an additional 4.8% show evidence of unstable main pulsation frequencies, which may be indicative of Blazhko periods longer than the time baseline of the observations (about four years). The Blazhko incidence rate we measure, which is only a lower limit, is somewhat higher than what has been found previously among RRab stars in the bulge, a fact that we attribute to the higher quality of our data set and the sensitivity of our search method. More strikingly, we have obtained a much higher ratio of BL2 stars (with symmetrical frequency triplets, i.e., one additional significant frequency on either side of the main pulsation frequency) to BL1 stars (with only a single additional significant frequency) than has been found previously. Within the limits of our sensitivity, we find BL2s to be about 1.7 times more common than BL1s, whereas previous studies of the bulge (Mizerski 2003) and the LMC (Alcock et

al. 2003) found BL2/BL1 incidence ratios of 0.59 and 0.83 respectively. Since we believe our detections of additional frequencies to be robust, we attribute this large increase of the BL2/BL1 ratio to the specific and very sensitive method we employ to detect additional, symmetrical frequency components. Furthermore, we have identified several instances of RRab stars that have two pairs of symmetrical frequency triplets, that is, stars with two separate sets of BL2 sidebands. These frequency quintuplets are unevenly spaced. This phenomenon may be important for understanding the long-unsolved origin of the Blazhko effect.

From the comparison of  $(V - I)_{ml}$  (minimum light) colors of bulge RR Lyrae stars, dereddened according to S04, with field RR Lyrae colors, we conclude that there is a discrepancy of 0.05–0.08 mag between the RR Lyrae-to-red clump (RC) color differential of the bulge population (measured from OGLE data) as compared to the local population. The sense of the effect is that the color separation is greater for the bulge population. We evaluate likely sources of systematic color errors and conclude that the color discrepancy is probably real. If this is correct then the most likely explanation seems to be the influence of metallicity on the color of the RC, or possibly the RR Lyrae, although there is some evidence against the latter possibility. We have observed a weak dependence of  $(V - I)_{0,ml}$  on period (redder at longer periods), but find no evidence of a further dependence on metallicity as estimated from the light curves. The trend with period cannot account for the observed color discrepancy. While the color discrepancy does not affect the conclusion that the reddening slope toward the bulge is anomalously flat, it does cast some doubt on the zero-point accuracy of S04’s reddening map. If the RR Lyrae are more reliable reddening tracers, then the  $E(V - I)$  values reported by S04 should be reduced by approximately 0.05 mag, with some variation from field to field as indicated in Table 4. We additionally measure an unexpectedly high star-to-star scatter of  $(V - I)_{0,ml}$  about 0.07 mag, which is larger than the photometric uncertainties and probably results from unresolved structure in the extinction or other random-type errors in the reddening map.

We exploit the approximately uniform mean  $V$ -band luminosities of the RRab stars to study the distance to and geometry of the inner Galaxy, and we compare these results to what S04 obtained from studying the RC. Since a coherent picture has not emerged, we summarize some relevant facts below.

- The Galactocentric distance modulus has been measured to be  $14.5 \pm 0.1$  mag by Eisenhauer et al. (2003) from the orbit of a star around the central black hole.
- Correcting for extinction according to S04, RC stars indicate a distance modulus to Baade’s Window (which should be virtually identical to the Galactocentric distance

modulus) of  $14.86 \pm 0.04$  mag, measured in the  $I$ -band, assuming that they have the same luminosities as local RC stars. Likely corrections to the reddening zero point (and concomitant corrections to the extinction, assuming that the measured reddening slopes hold all the way to  $E(V - I) = 0$ , for which there is no direct observational evidence) have the wrong sign to bring the distance modulus down.

- The distance modulus to Baade’s Window measured from RRab stars is somewhere between approximately 14.4–14.8 mag, depending mainly on the absolute magnitude calibration adopted. This is measured in the  $V$  band.
- Both the RC and the RR Lyrae stars clearly reveal the signature of the Galactic bar in fields with Galactic longitude  $|l| < 3$ . While the sense of the effect is the same (brighter at positive longitude as compared to negative longitude), the slopes are different. The magnitude difference from  $l \approx -3^\circ$  to  $l \approx 3^\circ$  is approximately 0.35–0.4 mag for the RC and 0.2–0.25 mag for the RR Lyrae.
- Both the RC and RR Lyrae magnitudes differ by 0.1–0.2 mag between fields approximately symmetrically located above and below the Galactic plane, with the fields at positive latitude being fainter. This assumes there is no significant extinction zero-point mismatch between the fields on opposite sides of the Galactic plane.
- There is a significant mismatch between the RC and RR Lyrae magnitude trends between about  $3^\circ < l < 10^\circ$ , increasing toward larger  $l$ , with the RR Lyrae becoming fainter and the RC becoming brighter; the discrepancy between the two trends reaches approximately 0.25 mag at  $l \approx 10^\circ$ .

### Acknowledgments

We are very pleased to acknowledge the countless helpful suggestions, interesting ideas and constant support of B. Paczyński. We also sincerely thank the OGLE team for their continuing efforts and generosity in sharing data.

### REFERENCES

- Alard, C., 1996, ApJ, 458, L17
- Alard, C., & Lupton, R., 1998, ApJ, 503, 325
- Alard, C., 2000, A&AS, 144, 363

- Alcock, C., et al., 1996, *AJ*, 111, 1146
- Alcock, C., et al., 1998, *ApJ*, 492, 190
- Alcock, C., et al., 2003, *ApJ*, 598, 597
- Alves, D.R., Rejkuba, M., Minniti, D., & Cook, K.H. 2002, *ApJ*, 573, L51
- Cacciari, C., & Clementini, G., 2003, astro-ph/0301550
- Day, A.S., et al., 2002, *PASP*, 114, 645
- Eisenhauer, F., Schödel, R., Genzel, R., Ott, T., Tecza, M., Abuter, R., Eckart, A., & Alexander, T., 2003, *ApJ*, 597, L121
- Gould, A. & Popowski, P., 1998, *ApJ*, 508, 844
- Guldenschuh, K.A., et al., 2005, *PASP*, 117, 721
- Jurcsik, J., & Kovács, G., 1996, *A&A*, 312, 111
- Kovács, G., & Zsoldos, E., 1995, *A&A*, 293, L57
- LaCluyzé, A., et al. 2004, *AJ*, 127, 1653
- Liu, T., & Janes, K.A. 1989, *ApJS*, 69, 593
- Mateo, M., Udalski, A., Szymański, M., Kaluzny, J., Kubiak, M., & Krzeminski, W., 1995, *AJ*, 109, 588
- Mizerski, T., 2003, *AcA*, 53, 307
- Moskalik, P., & Poretti, E. 2003, *A&A*, 398, 213
- Paczyński, B., & Stanek, K., 1998, *ApJ*, 494, L219
- Popowski, P., 2000, *ApJ*, 528, L9
- Press, W.H., Teukolsky, S.A., Vetterling, W.T., & Flannery, B.P. 1989, *Numerical Recipes in C* (2d ed.; Cambridge; Cambridge University Press)
- Roberts, D.H., Lehár, J., & Dreher, J.W., 1987, *AJ*, 93, 968
- Smith, H.A., 1995, *RR Lyrae Stars* (Cambridge, UK: Cambridge University Press)
- Smolec, R.. 2005, *AcA*, 55, 59

- Soszyński, I., et al., 2002, *AcA*, 52, 369
- Soszyński, I., et al., 2002, *AcA*, 53, 93
- Stellingwerf, R.F., 1978, *ApJ*, 224, 953
- Sturch, C. 1966, *ApJ*, 143, 774
- Stutz, A., Popowski, P., & Gould, A., 1999, *ApJ*, 521, 206
- Sumi, T., 2004, *MNRAS*, 349, 193 (S04)
- Sumi, T., et al. 2006, *ApJ*, 636, 240 (in press; astro-ph/0502363)
- Szymański, M.K., 2005, *AcA*, 55, 43
- Udalski, A., et al., 2002, *AcA*, 52, 217 (U02)
- Udalski, A., 2003, *ApJ*, 590, 284
- Walker, A.R., & Terndrup, D.M., 1991, *ApJ*, 378, 119
- Woźniak, P.R., Udalski, A., Szymański, M., Kubiak, M., Pietrzyński, G., Soszyński, I., & Żebruń, K., 2002, *AcA*, 52, 129

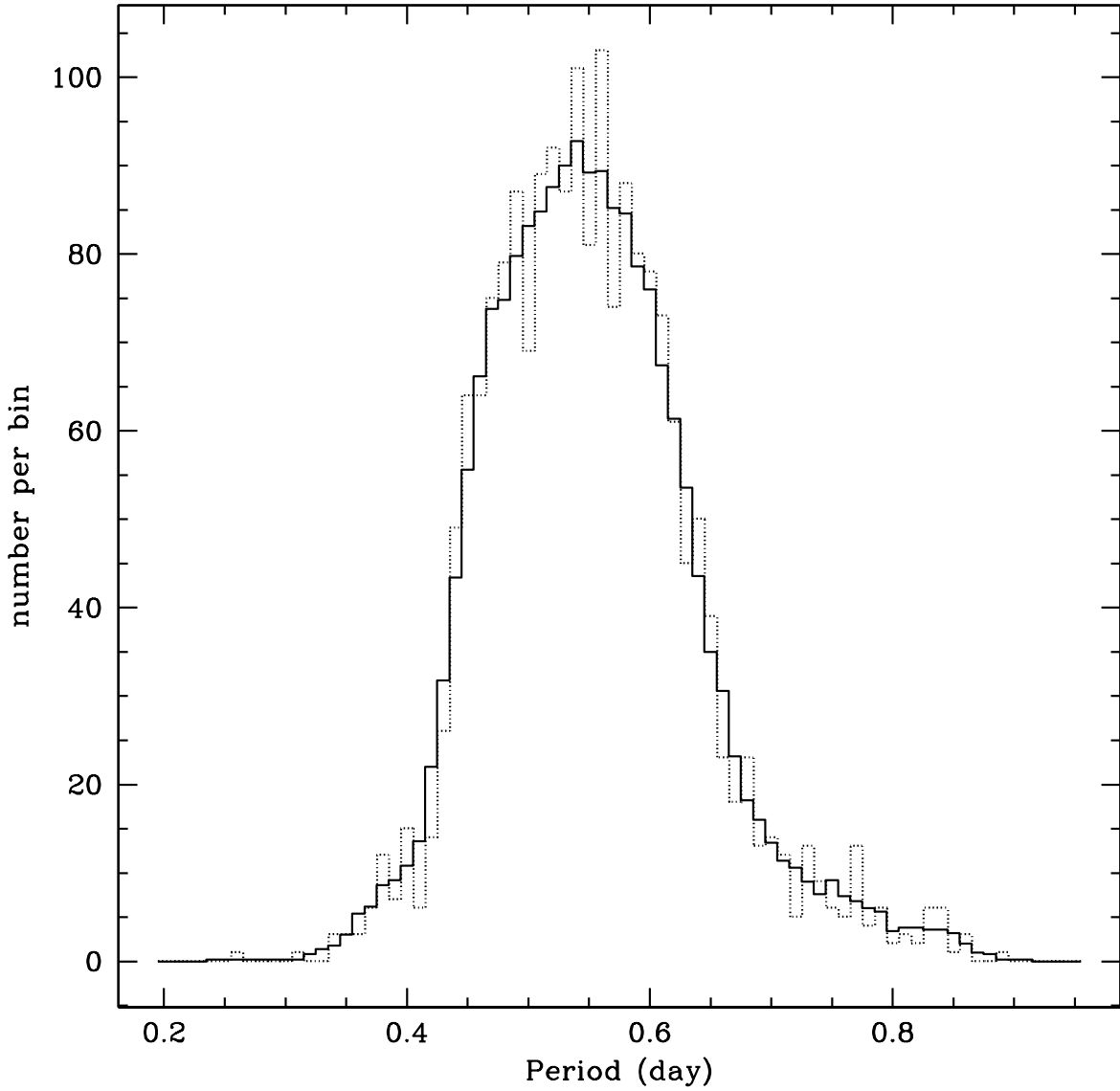


Fig. 1.— Period distribution of the 1913 stars in our sample. The light histogram is the observed distribution with a bin size of 0.01 day. The dark histogram is the result of smoothing the observed distribution with a five-bin boxcar filter.

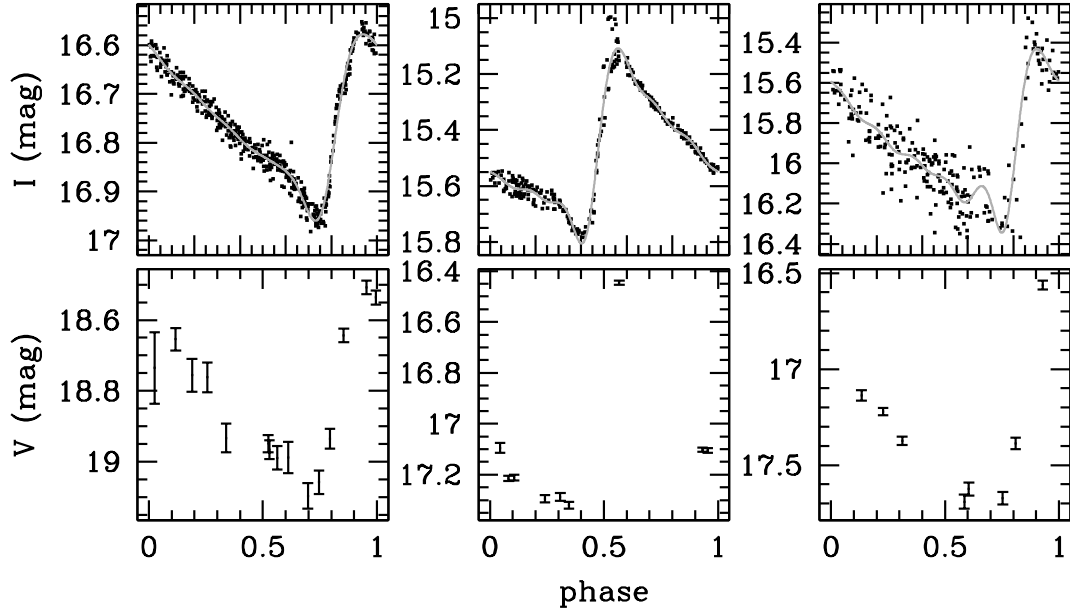


Fig. 2.— Example  $V$  and  $I$  light curves, with 6-harmonic Fourier model  $I$  light curves shown. From left to right: sc4-579960, a plain vanilla RRab star; sc34-208801, a Blazhko star; sc36-709901, an RRab star showing significant scatter in the light curve of an unknown nature. Error bars have been omitted from the upper panels for the sake of clarity, and are typically at the level of 0.01–0.02.



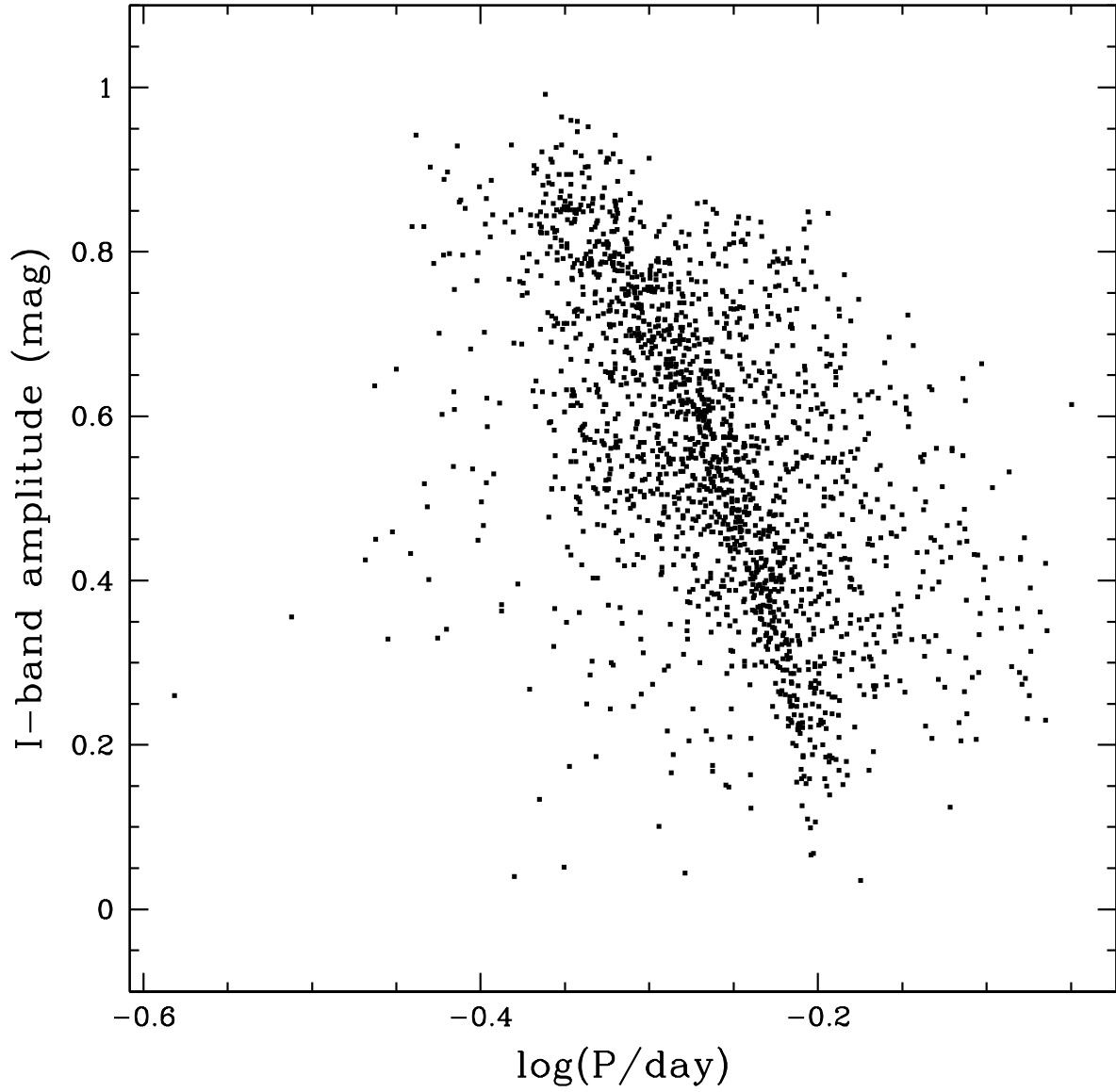


Fig. 3.— Bailey diagram for our RRab sample. As discussed in §4.2, nine stars in our sample fall above the vertical scale ( $> 1.1$  mag), likely because of blending-related calibration errors. The stars with the lowest amplitudes ( $< 0.1$  mag) are also probably blends.

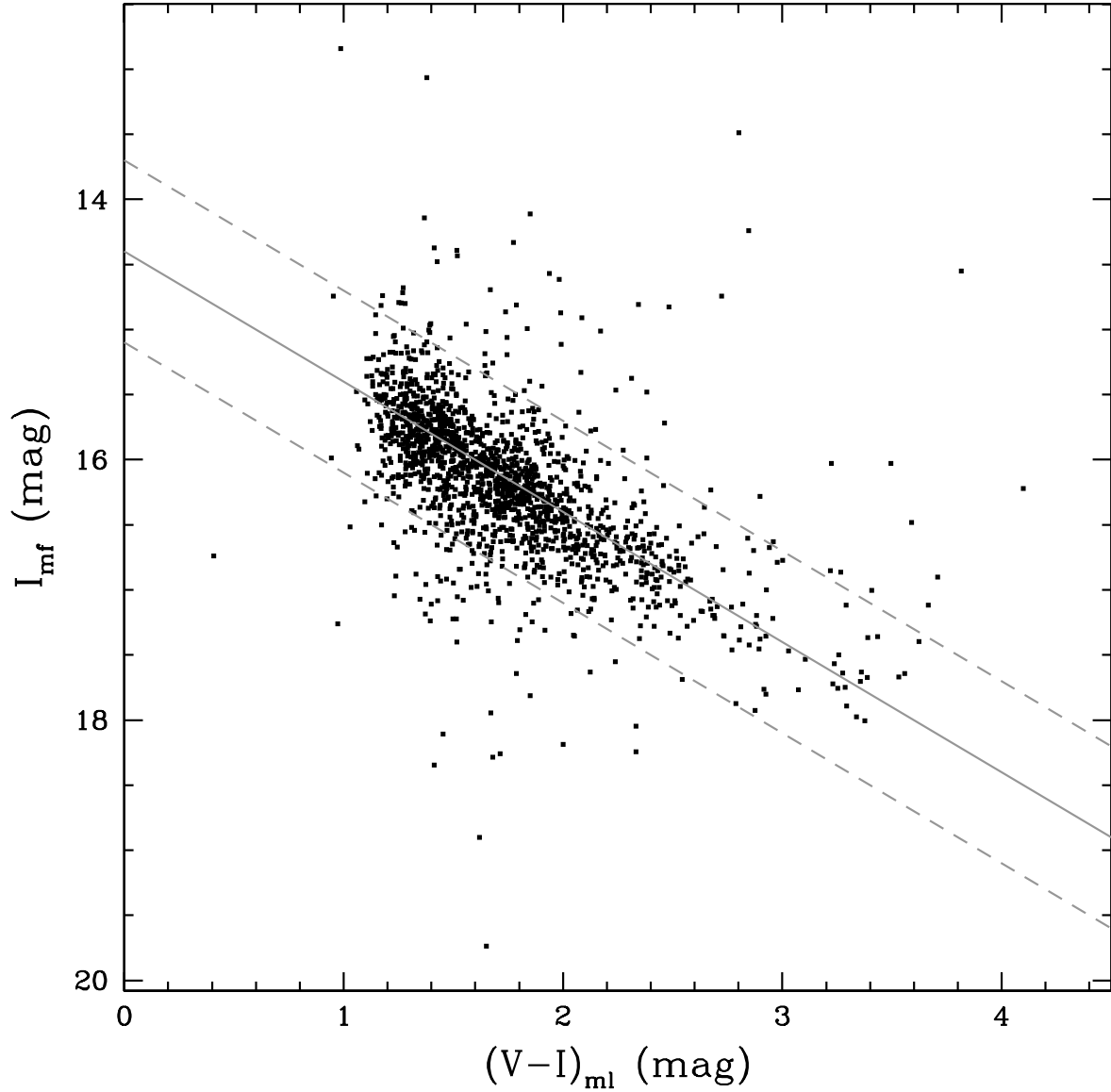


Fig. 4.— Observed color magnitude diagram for RR Lyrae stars in terms of the minimum light color  $(V - I)_{ml}$  and the magnitude at mean flux  $I_{mf}$ . The three over-plotted lines have slopes equal to unity (consistent with the range of measured reddening slopes). Stars falling outside the region between the dashed lines are excluded from the analysis in §5 as described in §5.1.

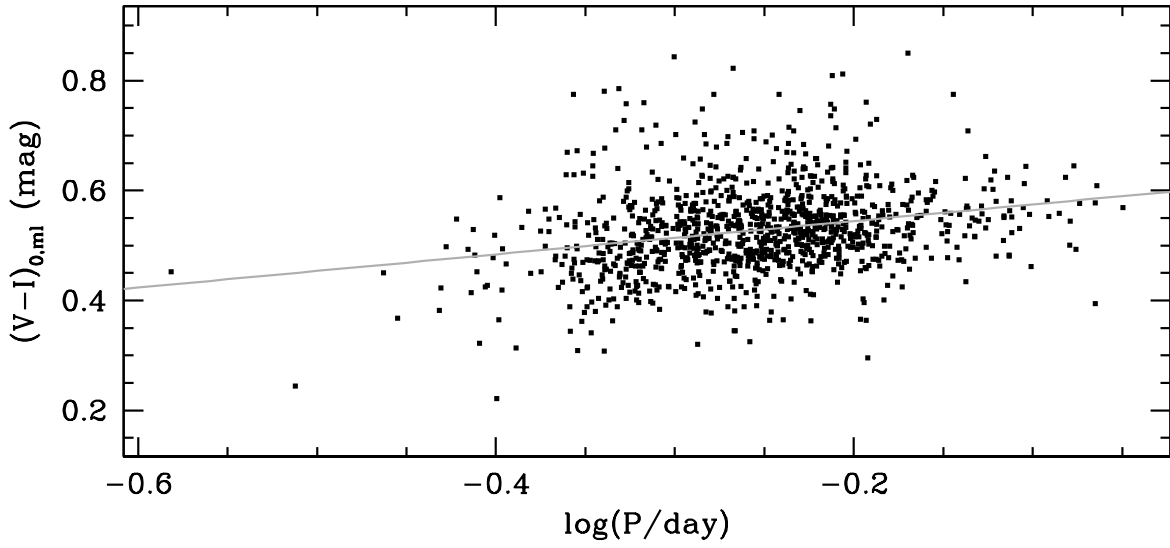


Fig. 5.— The correlation between  $\log P$  and dereddened, minimum light  $V - I$  color. Error bars have been omitted for clarity, but are typically at the level of 0.05 in  $V - I$  and negligible in  $\log P$ . The fit line shown was determined from an unweighted linear regression and does not depend sensitively on the inclusion of the two points with  $\log P < -0.5$ .

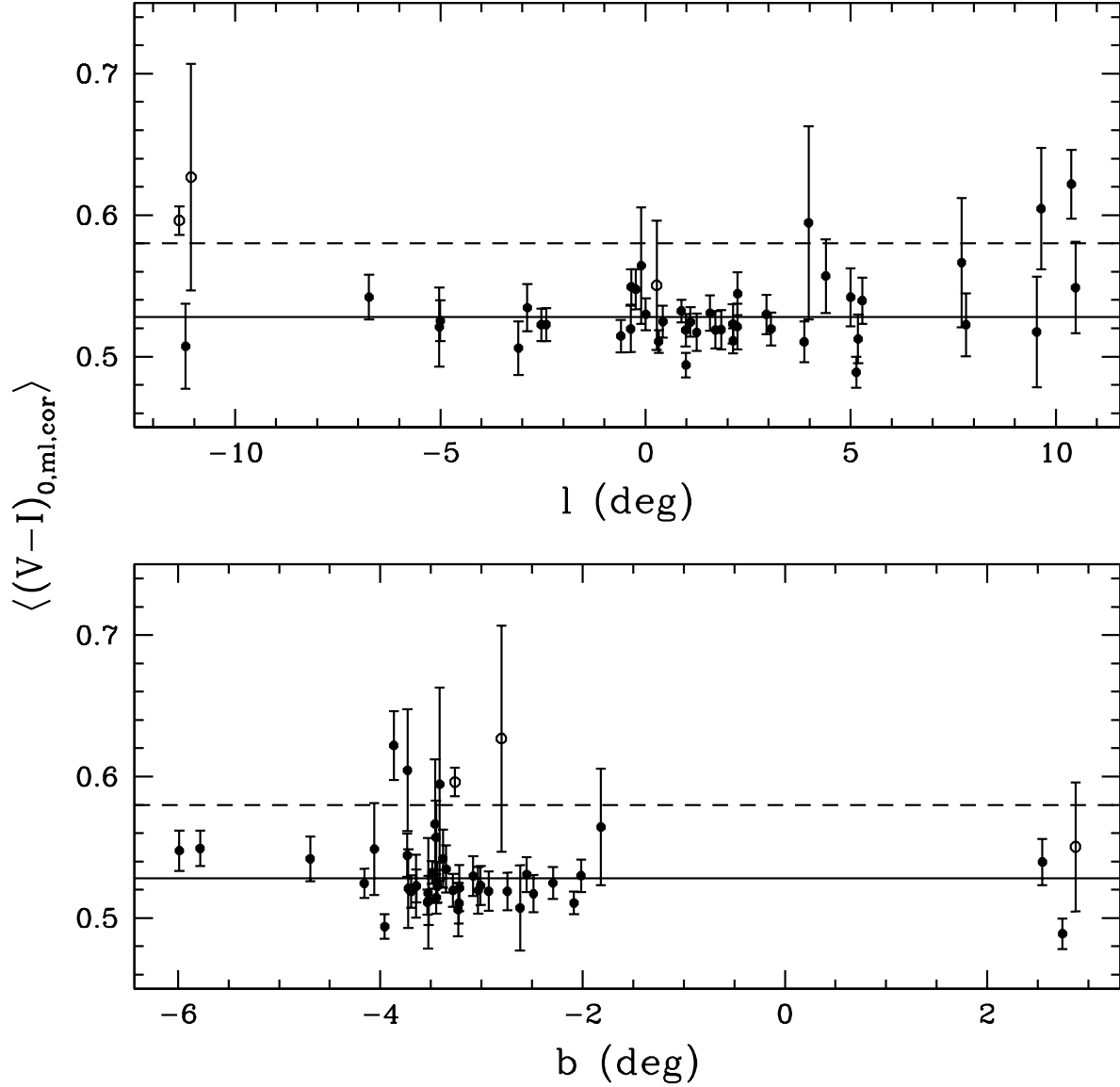


Fig. 6.— Mean  $(V - I)_{0,ml,cor}$  colors versus Galactic coordinates on a field-by-field basis. Open circles indicate that the corresponding field has less than 5 RR Lyrae which yielded usable color measurements. The solid horizontal line indicates the sample mean of 0.528; the dashed horizontal line at 0.58 indicates the mean color of local RR Lyrae stars from Guldenschuh et al. (2005).

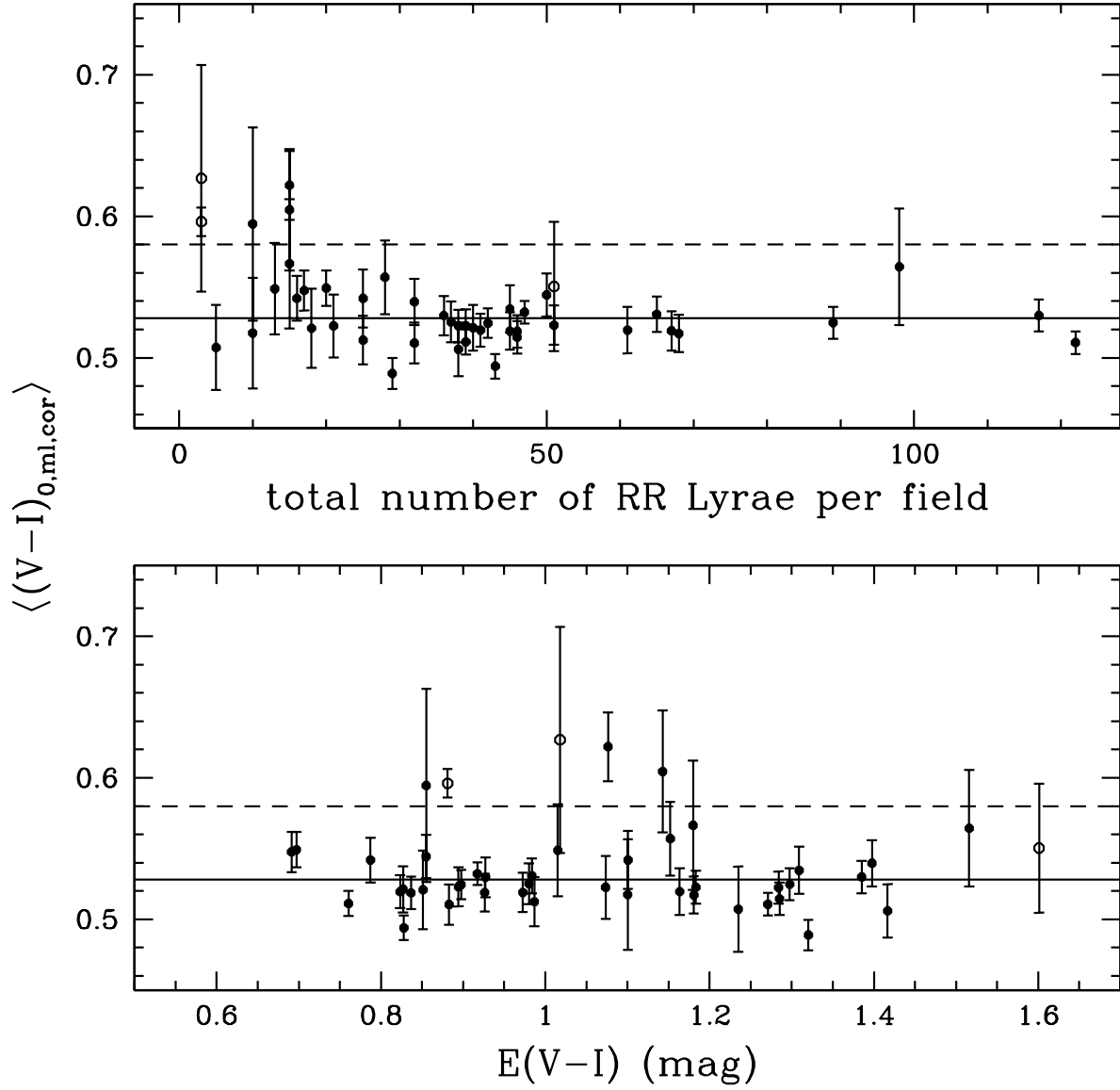


Fig. 7.— Mean  $(V - I)_{0,ml,cor}$  colors versus the total number of RR Lyrae (top panel) and the average reddening (bottom panel) on a field-by-field basis. The symbolic scheme and the horizontal lines are identical to those in Figure 6.

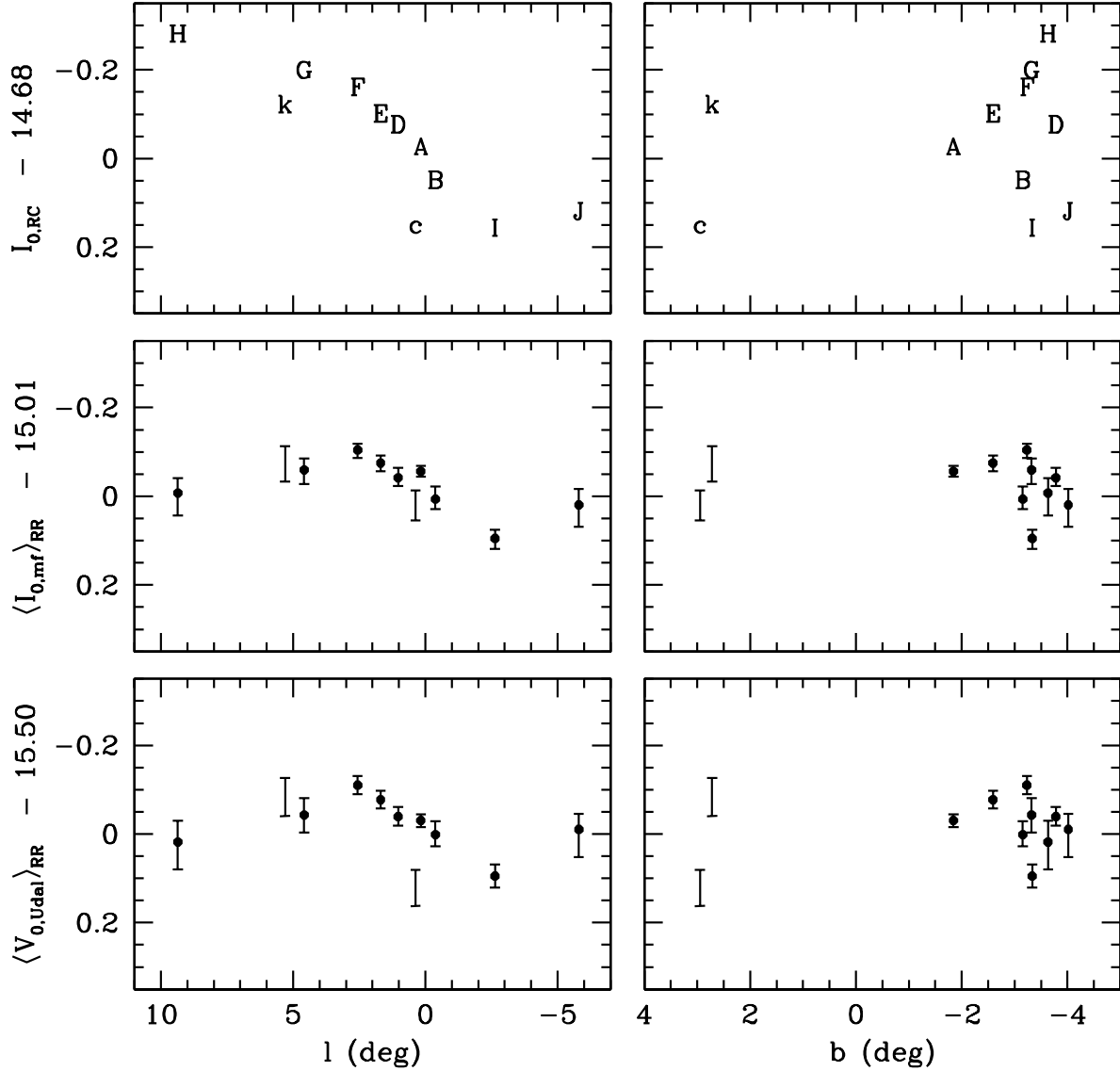


Fig. 8.— Mean extinction corrected magnitudes of RCGs ( $I$ -band, top panels; from S04) and RR Lyrae stars ( $I$ -band, middle panels;  $V$ -band, lower panels) as functions of Galactic longitude (left panels) and latitude (right panels), grouped into regions A–K as defined by S04. The zero points approximately correspond to the mean magnitudes at  $l = 0$ . The statistical errors on the points in the upper panels are typically less than 0.01 mag, smaller than the symbols. The regions ‘c’ and ‘k’ (shown in lower case in the upper panels and as error bars without points in the middle and lower panels), which are the only regions lying at positive Galactic latitudes, differ from the longitudinal trends evidenced by the remaining regions. The bar structure is clearly visible in the inner ( $|l| < 3$ ) regions of the left-hand panels, though differences between the RCG and RR Lyrae magnitude offsets are apparent.

Table 1. RRab sample.

field BUL_SC (1)	ID (2)	$\alpha_{2000}$ (hours) (3)	$\delta_{2000}$ (deg) (4)	Period (day) (5)	$I_{mf}$ (mag) (6)	Amp. (mag) (7)	N(I) (8)	$\chi^2/\nu$ (9)	$V$ (mag) (10)	$(V - I)_{ml}$ (mag) (11)	$A_V$ (mag) (12)	$A_I$ (mag) (13)	label (14)	noise (mmag) (15)	multID (16)
1	190423	18.04199	-30.4199	0.43308	15.73	0.63	232	40.1	16.83	1.29±0.14	1.52	0.75	BL2	14.7	...
1	566234	18.05063	-30.3314	0.56371	16.16	0.35	233	58.6	17.51	1.39±0.10	1.64	0.80	BL2+?	17.6	...
1	576932	18.04904	-30.3100	0.68769	15.69	0.36	253	2.0	16.98	1.42±0.04	1.70	0.83	...	3.3	...
1	587412	18.04701	-30.2152	0.49277	16.10	0.59	251	21.4	17.26	1.34±0.08	1.68	0.83	BL2	14.8	...
1	36798	18.03571	-30.2014	0.59743	15.84	0.29	251	4.8	17.34	1.50±0.02	1.72	0.85	BL2	4.2	...
1	410183	18.04384	-30.2007	0.59381	15.52	0.36	252	2.2	16.75	1.36±0.02	1.58	0.78	...	3.2	...
1	421285	18.04672	-30.1716	0.51940	15.91*	0.39	254	17.3	17.22	1.27±0.07	1.73	0.85	BL2	9.9	...
1	597902	18.04754	-30.1651	0.68050	15.81	0.19	252	1.2	17.25	1.49±0.03	1.87	0.92	...	2.7	...
1	608436	18.04774	-30.1342	0.61593	15.91	0.21	252	7.6	17.31	1.42±0.04	1.66	0.82	BL1	4.9	...
1	431836	18.04421	-30.1187	0.59450	15.90	0.34	242	6.7	17.25	1.41±0.10	1.70	0.83	BL1	12.1	...
1	59340	18.03466	-30.1023	0.50249	15.76	0.78	250	7.9	17.43	1.59±0.05	1.96	0.97	...	12.5	...
1	59700	18.03554	-30.1069	0.50791	16.30	0.66	251	26.9	17.87	1.62±0.03	2.06	1.01	PC	22.2	...
1	59431	18.03774	-30.0859	0.49027	16.11	0.65	251	25.7	17.34	1.32±0.11	1.79	0.88	BL2	14.8	...
1	619252	18.05103	-30.0667	0.46509	16.96	0.57	202	8.6	18.15*	1.38±0.10	1.47	0.72	PC	24.5	...
1	268899	18.03951	-30.0087	0.47363	16.03	0.81	251	4.6	17.27	1.30±0.03	1.61	0.79	...	3.7	...
1	452435	18.04316	-30.0038	0.46722	16.01	0.77	250	5.2	17.37	1.26±0.04	1.50	0.73	...	5.5	...
1	629186	18.04859	-29.9993	0.47863	15.80	0.86	251	8.9	16.89	1.25±0.04	1.50	0.74	...	4.8	...
1	629168	18.04927	-30.0017	0.55032	15.88	0.48	250	17.4	17.02	1.21±0.05	1.48	0.72	...	19.5	...
1	269030	18.04235	-29.9823	0.49502	15.70	0.57	252	228.7	16.95	1.38±0.20	1.44	0.71	PC	50.7	...
1	452510	18.04262	-29.9895	0.55213	15.82	0.53	252	3.9	17.02	1.19±0.02	1.38	0.68	BL1	5.1	...
1	452200	18.04311	-29.9887	0.82207	14.99	0.29	252	1.7	16.26	1.27±0.02	1.40	0.69	...	2.0	...
1	452506	18.04626	-29.9898	0.55722	15.56	0.51	246	2.8	16.69	1.23±0.03	1.33	0.65	...	4.0	...
1	280334	18.03862	-29.9486	0.49635	16.37	0.73	250	2.3	17.75	1.41±0.05	1.78	0.87	...	5.4	...
1	91419	18.03720	-29.9312	0.44857	16.18	0.86	251	6.3	17.36	1.39±0.04	1.72	0.84	...	7.0	...
1	463376	18.04528	-29.9054	0.44442	15.76	0.81	201	6.5	17.12*	1.22±0.04	1.42	0.69	...	5.8	...
1	291846	18.03947	-29.8939	0.45411	15.82	0.79	252	9.3	16.97	1.29±0.04	1.60	0.78	...	4.5	...
1	652490	18.05015	-29.8977	0.55453	15.21	0.57	251	4.0	16.32	1.14±0.02	1.30	0.64	PC	5.1	...
1	474984	18.04581	-29.8856	0.60023	15.69	0.48	228	2.2	16.91	1.32±0.02	1.55	0.76	...	4.4	...
1	474747	18.04416	-29.8656	0.52955	15.69	0.64	247	22.6	16.71	1.30±0.02	1.52	0.75	BL2	11.8	...
1	116187	18.03639	-29.8346	0.61174	15.84	0.30	247	1.4	17.07	1.27±0.03	1.49	0.73	...	3.2	...
1	665317	18.04934	-29.8108	0.42413	15.64	0.75	251	31.8	16.76	1.27±0.06	1.38	0.68	BL1	14.7	...
1	130494	18.03560	-29.7847	0.48306	15.88	0.79	251	5.2	17.15	1.31±0.04	1.64	0.80	...	8.2	...
1	130531	18.03746	-29.7788	0.35476	16.06*	0.66	251	3.0	17.56	1.51±0.04	1.54	0.76	...	5.1	...
1	130718	18.03502	-29.7495	0.63271	15.92	0.42	249	12.1	17.35	1.42±0.05	1.43	0.70	BL?	6.5	...
1	317844	18.04071	-29.7296	0.49322	15.54	0.71	251	5.4	16.92	1.28±0.02	1.39	0.68	...	4.7	...
1	678325	18.04711	-29.7389	0.42179	16.15	0.76	251	2.6	17.20	1.14±0.03	1.35	0.67	PC	5.8	...
1	144336	18.03765	-29.7049	0.42434	15.97	0.78	250	6.0	17.26	1.26±0.05	1.49	0.73	...	6.2	...
1	144492	18.03646	-29.6825	0.40112	16.02	0.87	249	8.9	17.22	1.22±0.04	1.56	0.77	...	7.9	...
1	144504	18.03719	-29.6803	0.47787	16.14	0.82	90	3.7	17.31	1.22±0.04	1.55	0.76	...	12.2	...
1	331128	18.04075	-29.6781	0.63828	15.46	0.22	252	1.3	16.71	1.35±0.02	1.54	0.76	...	3.4	...
1	512310	18.04424	-29.6729	0.66002	15.90	0.56	242	1.7	17.31	1.44±0.02	1.89	0.93	...	3.9	...
1	700895	18.04823	-29.6463	0.45696	15.59	0.42	250	1.4	16.93	1.31±0.01	1.63	0.80	...	3.2	...
1	169019	18.03426	-29.5863	0.55208	16.30	0.63	230	2.3	17.84	1.47±0.06	2.26	1.11	...	7.0	...
1	168859	18.03648	-29.5699	0.56632	15.82	0.47	249	2.2	17.09	1.30±0.02	1.84	0.90	...	4.8	...
1	366334	18.03906	-29.5067	0.48692	16.67	0.62	247	27.3	18.64	2.05±0.09	2.78	1.36	BL2	26.1	...
1	366819	18.03967	-29.5059	0.53524	17.06	0.40	246	9.6	19.20	2.14±0.06	2.82	1.38	BL2	18.5	...
2	425494	18.07648	-29.3191	0.75001	15.42	0.27	234	1.1	16.75	1.31±0.02	1.50	0.74	...	2.4	...
2	464	18.06687	-29.3052	0.50933	15.40	0.52	234	2.7	16.65	1.18±0.02	1.38	0.68	...	4.4	...
2	436452	18.07862	-29.2820	0.59032	14.68	0.48	235	8.1	15.93	1.27±0.03	1.50	0.74	...	4.5	...
2	436573	18.07838	-29.2569	0.49512	15.77	0.51	233	68.1	16.96	1.30±0.08	1.64	0.80	BL2	20.0	...

Note. — Columns two, three, four and ten are from U02. Column six gives the magnitude at mean flux, column seven gives the minimum-to-maximum  $I$ -band amplitude, and column nine gives  $\chi^2$  per degree of freedom; all these quantities are derived from 6-harmonic Fourier models (see §4.2). An asterisk in column six or ten indicates that the photometry may be unreliable as assessed in §2. Column eight gives the number of  $I$ -band observations. Typical errors (not shown) for the quantities in columns five, six and seven are approximately: less than  $10^{-5}$  day, 0.005 mag and 0.02 mag. Columns 12 and 13 are from Sumi (2004). Column 14 indicates the classification, and column 15 gives the approximate noise level in the Blazhko range, as described in §4.1. For stars detected in two overlapping fields, column 16 provides a unique number from 1–25 to identify the matching data set. (The complete version of this table will appear electronically.)

Table 2. RRab candidates rejected from the sample.

field BUL_SC (1)	ID (2)	$\alpha_{2000}$ (hours) (3)	$\delta_{2000}$ (deg) (4)	flag (5)
3	507991	17.89574	-30.0205	2
3	536371	17.89554	-29.8880	2
4	454331	17.91266	-29.9422	2
4	59232	17.90324	-29.9089	4
4	93538	17.90302	-29.7675	3
4	108677	17.90510	-29.6869	3
20	548861	17.99151	-28.6643	2
21	471290	18.00916	-29.3047	2
22	410981	17.94948	-31.1071	2
22	176263	17.93831	-30.3981	3
27	443264	17.80931	-35.1738	2
27	640784	17.81499	-34.9702	3
28	116982	17.78153	-37.4575	3
28	327437	17.79315	-37.3613	3
28	136056	17.78086	-37.2941	3
28	142101	17.78285	-37.2114	3
28	142130	17.78419	-37.2014	3
28	346566	17.79030	-37.1777	3
28	43959	17.77705	-37.1680	3
28	346511	17.79238	-37.1371	3
28	260827	17.78959	-37.0154	3
28	64509	17.77878	-36.9898	3
28	77184	17.77991	-36.8848	3
28	380745	17.79189	-36.8554	3
28	380822	17.79203	-36.8366	3
30	634223	18.02836	-29.0187	2
30	352519	18.02028	-28.5756	3
31	562207	18.04094	-28.3241	3
33	130969	18.08350	-28.7448	2
34	298657	17.96759	-29.4475	3
34	682061	17.97475	-28.8035	2
34	703555	17.97453	-28.7290	2
37	55168	17.86717	-30.0903	3
37	405002	17.87823	-29.9921	2
37	440744	17.87862	-29.8314	2
37	473842	17.87864	-29.5821	2
39	684442	17.93639	-29.7803	2
40	479913	17.85459	-32.7850	3
41	316456	17.87206	-33.5204	3
45	356751	18.06310	-30.4038	2
45	245930	18.05976	-30.0334	1
45	245283	18.05976	-30.0339	1
45	254862	18.05998	-30.0311	3

Note. — Column two gives the star catalog number from U02. Column five indicates why the star was rejected: if there were less than 25 good data points in the *I*-band the flag was incremented by +1, if the light curve was visually inconsistent with an RRab light curve (e.g., constant) the flag was incremented by +2, and if the star was blended with a true RRab star the flag was incremented by +4.



Table 3. Blazhko stars.

field	ID	label	noise	limit	$\Delta f_1$	$\mathcal{A}_1$	$\Delta f_2$	$\mathcal{A}_2$	$\Delta f_3$	$\mathcal{A}_3$	$\Delta f_4$	$\mathcal{A}_4$	$\Delta f_5$	$\mathcal{A}_5$
BUL_SC	(2)	(3)	(mmag)	(mmag)	( $10^{-3}d^{-1}$ )	(mmag)	( $10^{-3}d^{-1}$ )	(mmag)	( $10^{-3}d^{-1}$ )	(mmag)	( $10^{-3}d^{-1}$ )	(mmag)	( $10^{-3}d^{-1}$ )	(mmag)
(1)			(4)	(5)	(6)	(7)	(8)	(9)	(10)	(11)	(12)	(13)	(14)	(15)
1	190423	BL2	14.7	...	30.4	28.8	-30.3	17.9	...	...	...	...	...	...
1	566234	BL2+7	17.6	...	0.6	49.6	35.2	44.7	-0.6	36.0	...	...	...	...
1	587412	BL2	14.8	...	14.6	38.2	-14.8	26.1	...	...	...	...	...	...
1	36798	BL2	4.2	...	16.5	16.0	-16.3	5.3	...	...	...	...	...	...
1	421285	BL2	9.9	...	17.2	20.9	-17.1	19.0	...	...	...	...	...	...
1	608436	BL1	4.9	2.3	21.5	24.4	...	...	...	...	...	...	...	...
1	431836	BL1	12.1	5.5	14.4	18.7	...	...	...	...	...	...	...	...
1	59700	PC	22.2	...	-0.7	29.7	...	...	...	...	...	...	...	...
1	59431	BL2	14.8	...	9.1	33.5	-9.2	24.6	...	...	...	...	...	...
1	619252	PC	24.5	...	-0.6	13.9	...	...	...	...	...	...	...	...
1	269030	PC	50.7	...	0.6	112.2	...	...	...	...	...	...	...	...
1	452510	BL1	5.1	5.1	45.9	12.8	...	...	...	...	...	...	...	...
1	652490	PC	5.1	...	0.5	4.8	...	...	...	...	...	...	...	...
1	474747	BL2	11.8	...	15.8	20.7	-16.0	16.5	...	...	...	...	...	...
1	665317	BL1	14.7	14.7	-22.5	29.3	...	...	...	...	...	...	...	...
1	130718	BL?	6.5	...	14.5	23.7	18.0	16.3	...	...	...	...	...	...
1	678325	PC	5.8	...	0.5	6.7	...	...	...	...	...	...	...	...
1	366334	BL2	26.1	...	-12.9	46.0	13.0	31.1	...	...	...	...	...	...
1	366819	BL2	18.5	...	22.4	40.7	-22.3	33.1	...	...	...	...	...	...
2	436573	BL2	20.0	...	-6.1	45.1	6.3	29.3	...	...	...	...	...	...
2	447803	BL?	9.7	...	-3.6	13.5	15.3	11.4	...	...	...	...	...	...
2	40061	PC	26.9	...	-0.7	28.6	...	...	...	...	...	...	...	...
2	459476	BL1	5.7	3.3	32.9	16.9	...	...	...	...	...	...	...	...
2	279494	BL2	5.1	...	-17.8	10.9	17.8	6.4	...	...	...	...	...	...
2	304657	BL2	11.3	...	-3.4	19.6	3.2	18.4	...	...	...	...	...	...
2	518211	BL1	3.4	3.6	16.5	19.2	...	...	...	...	...	...	...	...
2	318604	BL2	19.1	...	23.5	52.7	-23.3	37.6	...	...	...	...	...	...
2	530487	BL1	18.0	18.0	-34.0	30.9	...	...	...	...	...	...	...	...
2	722091	BL1	7.8	6.1	20.7	22.9	...	...	...	...	...	...	...	...
2	733835	BL1	54.7	54.7	-2.3	38.0	...	...	...	...	...	...	...	...
2	135403	BL?	15.4	...	49.6	32.4	1.1	19.8	...	...	...	...	...	...
2	345581	PC	5.5	...	0.5	6.8	...	...	...	...	...	...	...	...
2	542801	BL2	7.2	...	38.7	14.4	-38.8	11.1	...	...	...	...	...	...
2	733728	BL?	53.6	...	25.1	73.9	-0.8	52.2	...	...	...	...	...	...
2	555864	BL1	6.1	3.3	6.3	19.6	...	...	...	...	...	...	...	...
2	581017	BL2+PC	15.0	...	17.7	30.9	0.6	12.0	-17.4	10.4	...	...	...	...
2	783422	BL2	15.6	...	12.9	25.3	-13.1	21.4	...	...	...	...	...	...
3	422608	BL1	17.1	17.1	25.1	46.4	...	...	...	...	...	...	...	...
3	216589	BL2	20.7	...	9.6	36.2	-11.9	20.3	...	...	...	...	...	...
3	422817	BL1	5.9	4.7	14.2	9.8	...	...	...	...	...	...	...	...

Note. — Columns one through four are reproduced from Table 1. Column five gives the largest amplitude observed inside the equidistant triplet frequency region, for the BL1 stars. Columns six through 15 list the significant frequencies detected within  $0.1 \text{ day}^{-1}$  of the main pulsation frequency and their amplitudes. All frequencies are in units of  $10^{-3} \text{ day}^{-1}$  and all amplitudes are in milli-magnitudes. (The complete version of this table will appear electronically.)

Table 4. RRAb numbers and colors on a field by field basis.

field BUL_SC	l (deg)	b (deg)	N(V-I) (4)	N(RR) (5)	$\langle(V-I)_{0,ml}\rangle$ (mag) (6)	$\langle(V-I)_{0,ml,cor}\rangle$ (mag) (7)	$\sigma_{cor}$ (mag) (8)	$\langle E(V-I)\rangle$ (mag) (9)
1	0.9791	-3.6962	37	46	0.516±0.012	0.519±0.011	0.068	0.837
2	2.1339	-3.5333	30	39	0.505±0.010	0.511±0.009	0.046	0.760
3	0.0064	-2.0142	65	117	0.535±0.011	0.530±0.011	0.090	1.385
4	0.3235	-2.0853	87	122	0.510±0.008	0.511±0.008	0.074	1.271
5	-0.3321	-1.4061	0	72	...	...	0.000	...
6	-0.3509	-5.7804	14	20	0.562±0.012	0.549±0.012	0.043	0.697
7	-0.2358	-5.9869	13	17	0.561±0.015	0.548±0.014	0.047	0.691
8	10.3770	-3.8657	9	15	0.629±0.023	0.622±0.024	0.064	1.076
9	10.4780	-4.0589	7	13	0.552±0.035	0.549±0.032	0.072	1.015
10	9.5332	-3.5262	5	10	0.514±0.035	0.517±0.039	0.068	1.100
11	9.6410	-3.7305	10	15	0.612±0.045	0.605±0.043	0.121	1.143
12	7.7018	-3.4585	7	15	0.569±0.046	0.566±0.046	0.102	1.180
13	7.8057	-3.6462	14	21	0.525±0.025	0.523±0.022	0.077	1.074
14	5.1346	2.7437	14	29	0.505±0.014	0.489±0.011	0.038	1.320
15	5.2809	2.5446	16	32	0.546±0.017	0.540±0.016	0.061	1.398
16	4.9966	-3.3797	13	25	0.548±0.017	0.542±0.021	0.068	1.101
17	5.1793	-3.5223	17	25	0.517±0.018	0.512±0.017	0.067	0.987
18	3.8671	-3.2227	20	32	0.506±0.016	0.510±0.014	0.061	0.883
19	3.9736	-3.4133	5	10	0.607±0.069	0.595±0.068	0.118	0.855
20	1.5724	-2.5531	44	65	0.534±0.013	0.531±0.012	0.080	0.984
21	1.7038	-2.7437	27	45	0.524±0.013	0.519±0.013	0.066	0.926
22	-0.3622	-3.0323	27	61	0.515±0.018	0.520±0.016	0.082	1.164
23	-0.6022	-3.4458	27	46	0.516±0.012	0.515±0.012	0.058	1.285
24	-2.5396	-3.4374	28	38	0.525±0.012	0.522±0.011	0.058	1.284
25	-2.4201	-3.6441	27	39	0.525±0.012	0.523±0.012	0.058	1.183
26	-5.0003	-3.4381	27	37	0.522±0.015	0.525±0.014	0.072	0.980
27	-5.0240	-3.7231	12	18	0.523±0.028	0.521±0.028	0.088	0.851
28	-6.8543	-4.5107	0	0	...	...	0.000	...
29	-6.7370	-4.6923	11	16	0.554±0.016	0.542±0.016	0.047	0.787
30	1.8436	-2.9276	49	67	0.525±0.014	0.519±0.014	0.095	0.973
31	2.1299	-3.0077	27	51	0.523±0.015	0.523±0.014	0.069	0.894
32	2.2353	-3.2179	30	40	0.519±0.016	0.521±0.016	0.086	0.827
33	2.2411	-3.7339	35	50	0.548±0.015	0.544±0.015	0.087	0.855
34	1.2466	-2.4852	51	68	0.517±0.014	0.517±0.013	0.092	1.181
35	2.9448	-3.0807	23	36	0.532±0.016	0.530±0.014	0.064	0.927
36	3.0602	-3.2802	31	41	0.523±0.012	0.520±0.012	0.062	0.823
37	-0.1047	-1.8190	7	98	0.560±0.037	0.564±0.041	0.092	1.516
38	0.8742	-3.4880	40	47	0.537±0.007	0.532±0.008	0.050	0.917
39	0.4221	-2.2934	56	89	0.527±0.012	0.525±0.011	0.083	1.297
40	-3.0962	-3.2304	20	38	0.500±0.020	0.506±0.019	0.080	1.417
41	-2.8799	-3.3503	24	45	0.538±0.015	0.535±0.017	0.078	1.309
42	4.3910	-3.4491	19	28	0.552±0.028	0.557±0.026	0.108	1.152
43	0.2705	2.8736	3	51	0.564±0.057	0.550±0.046	0.046	1.601
44	-0.5268	-1.2732	0	28	...	...	0.000	...
45	0.9857	-3.9573	38	43	0.498±0.010	0.494±0.009	0.053	0.828
46	1.0943	-4.1578	32	42	0.530±0.011	0.524±0.010	0.057	0.898
47	-11.2050	-2.6179	5	5	0.517±0.022	0.507±0.030	0.052	1.235
48	-11.0759	-2.8024	1	3	0.647±0.080	0.627±0.080	...	1.018
49	-11.3595	-3.2618	2	3	0.593±0.033	0.596±0.010	0.010	0.881

Note. — Columns four and five list, for each field, the number of RR Lyrae that yielded a usable measurement of  $(V-I)_{ml}$  and the total number of RR Lyrae in our catalog. Column eight gives the standard deviation of  $\langle(V-I)_{0,ml,cor}\rangle$ .